

Cosmic Alchemy:

*The Origin of the
Chemical Elements*

Eric Norman

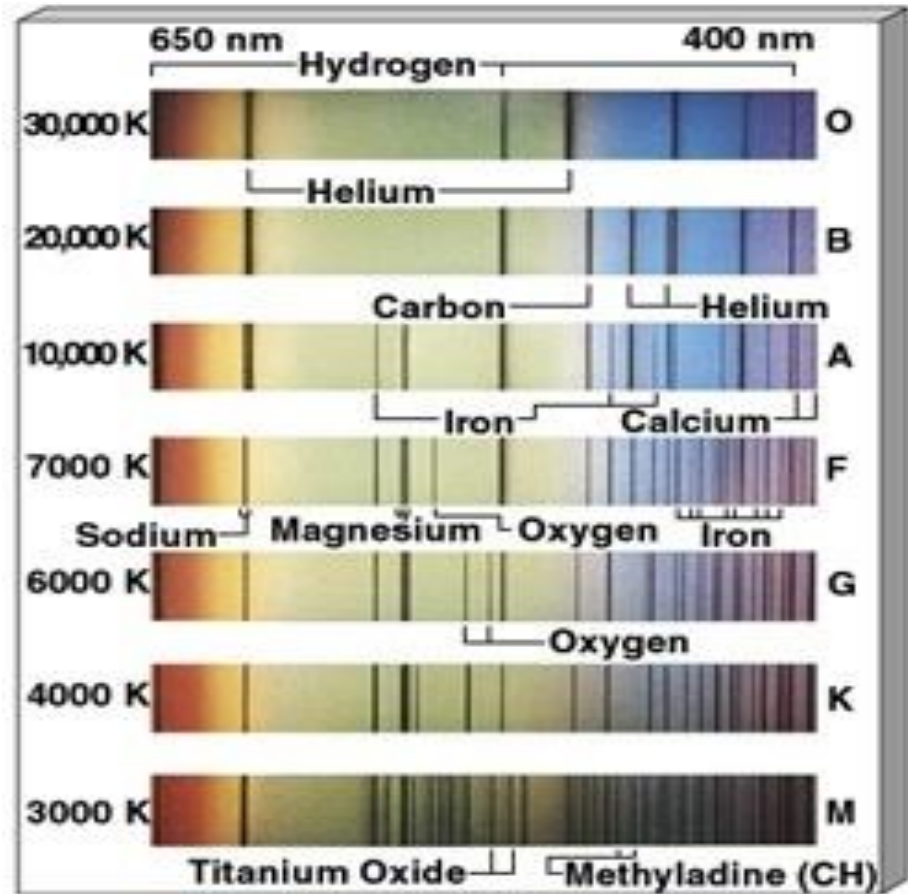
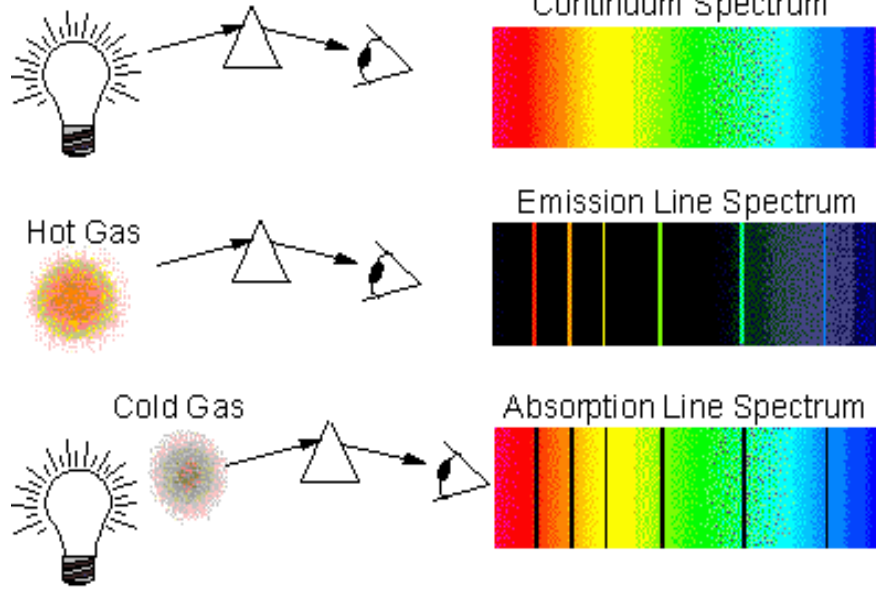
Nuclear Engineering Dept.

Univ. of California at Berkeley

Dark Night Sky



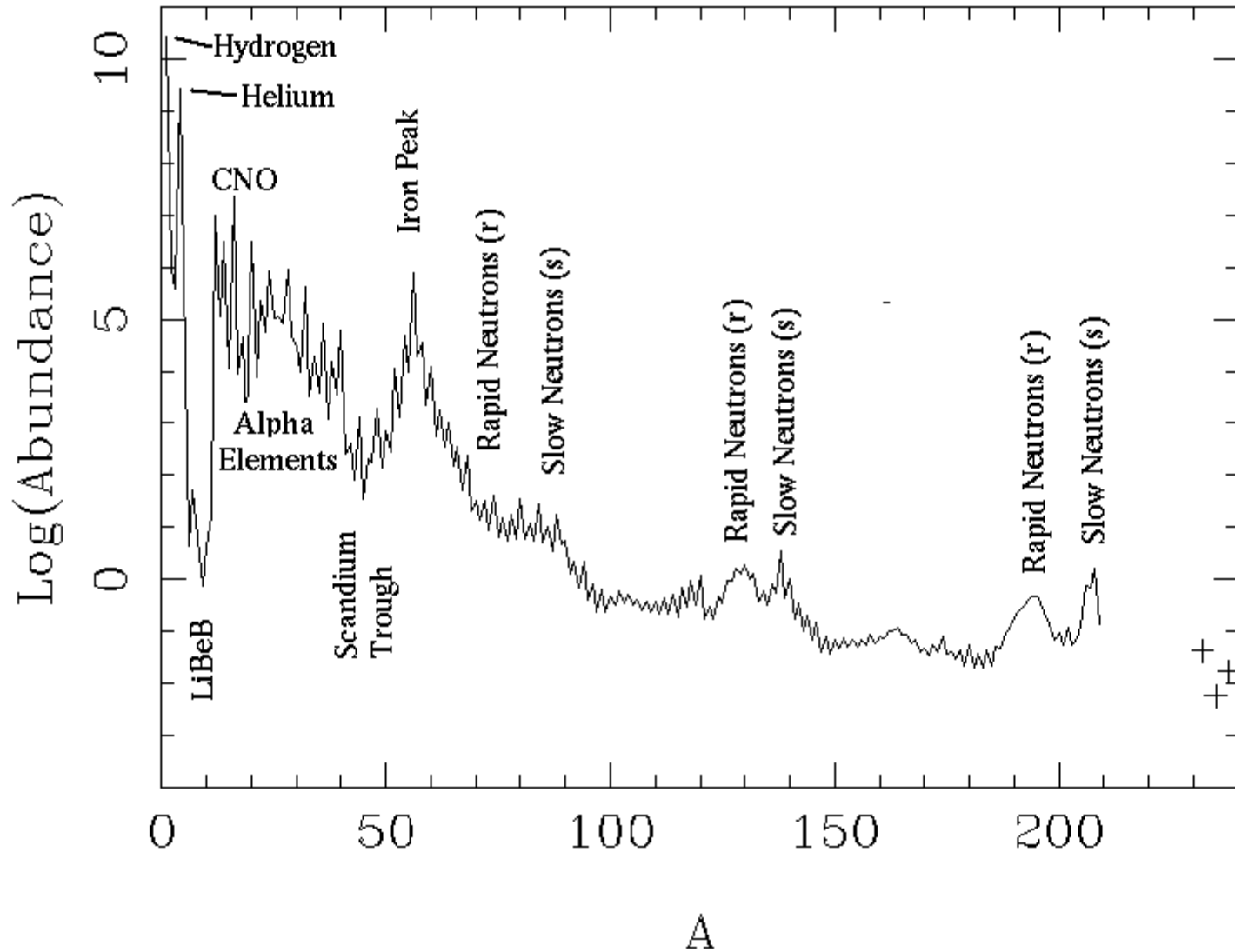
Visible EM Spectrum



What is the universe made of ?

- **Hydrogen = 75%, by mass**
- **Helium = 23 %**
- **Everything Else = 2%**

Standard Abundance Distribution (SAD) vs. A



Evidence for Big Bang

- 1. Expansion of the universe**
- 2. Cosmic microwave background**
- 3. Light element abundances**

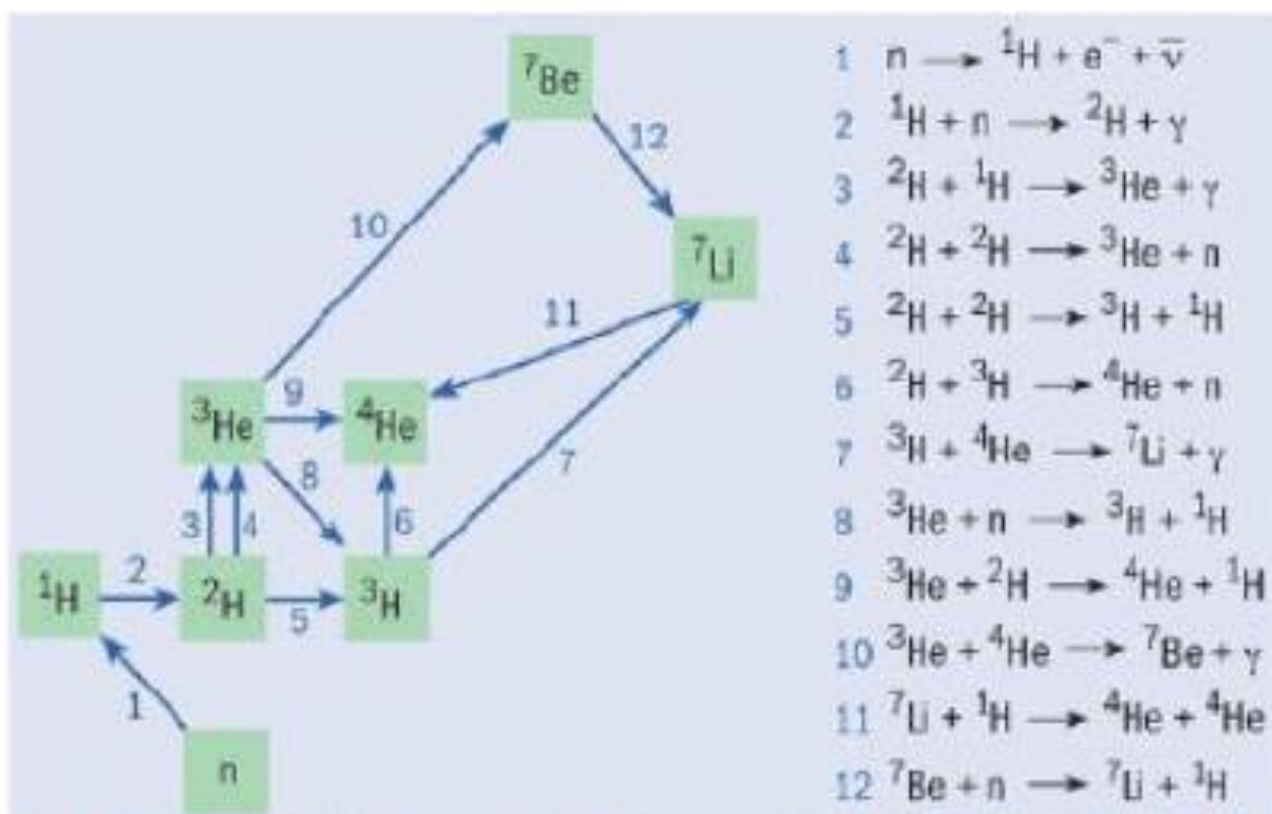
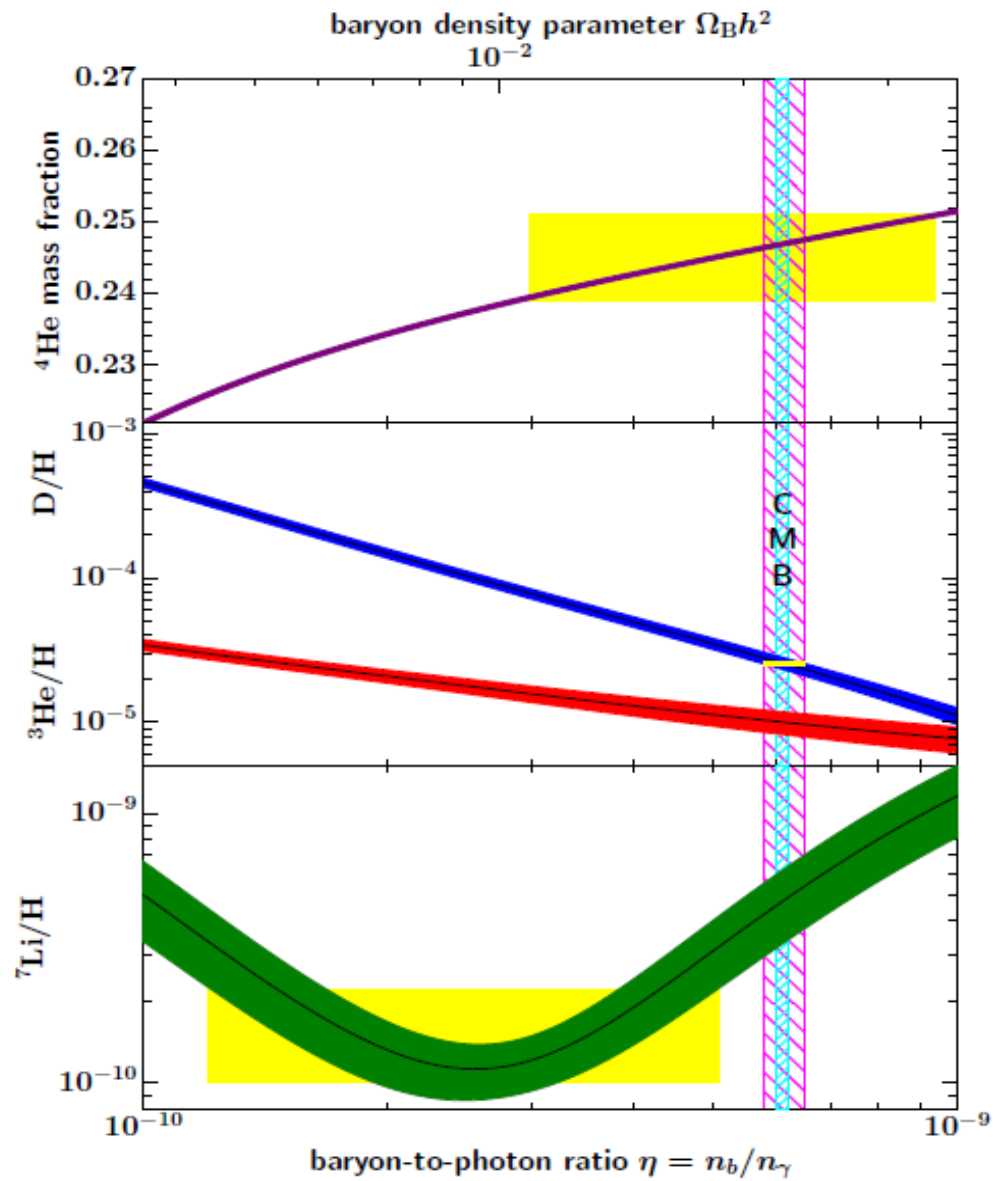


Figure 1: Nuclear reactions - http://physicsworld.com/cws/article/print/30680/1/PWfea4_08-07

Benjamin Topper

Lack of stable $A = 5$ or $A = 8$ nuclei prevents heavy element production in Big Bang

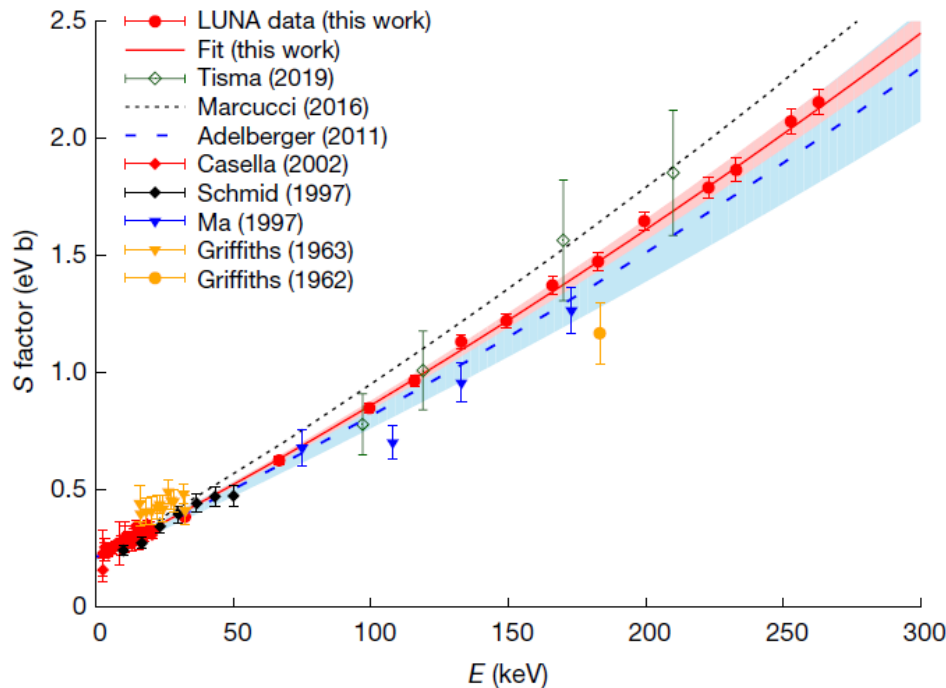


**Particle
Data
Group
2020**

Figure 24.1: The primordial abundances of ${}^4\text{He}$, D , ${}^3\text{He}$, and ${}^7\text{Li}$ as predicted by the standard model of Big-Bang nucleosynthesis — the bands show the 95% CL range [47]. Boxes indicate the observed light element abundances. The narrow vertical band indicates the CMB measure of the cosmic baryon density, while the wider band indicates the BBN $\text{D}+{}^4\text{He}$ concordance range (both at 95% CL).

Recent results from LUNA collaboration

Nature **587** (2020) 210



S-factor for the
 $d(p,\gamma)^3\text{He}$ reaction

Table 1 | Mean values and 68% confidence level ranges for $\Omega_b h^2$ (with relative uncertainties δ) and N_{eff}

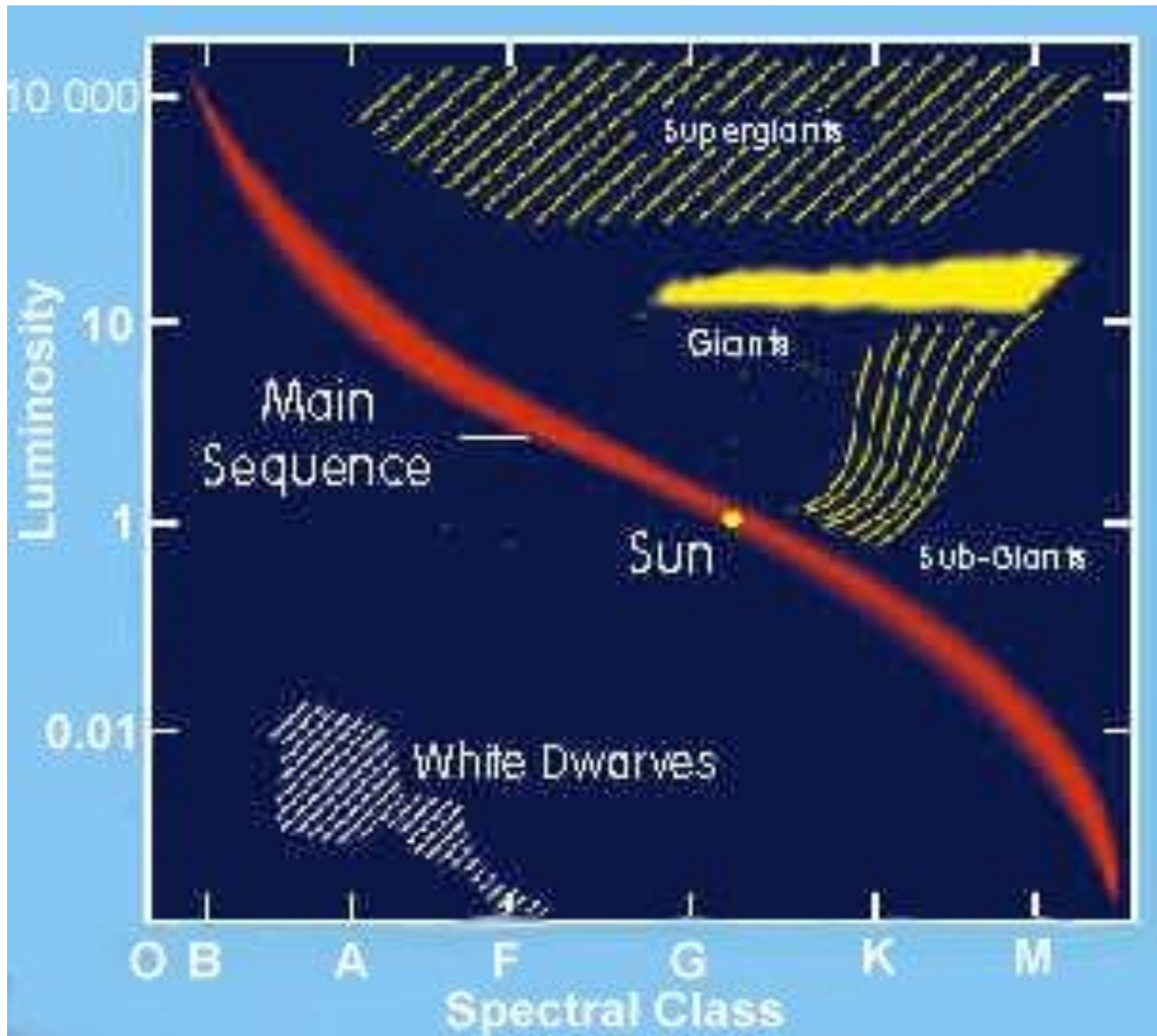
	$\Omega_b h^2$	δ (%)	N_{eff}
D + 3 ν (without LUNA data)	0.02271 ± 0.00062	2.73	3.045
D + 3 ν (with new LUNA data)	0.02233 ± 0.00036	1.61	3.045
CMB + 3 ν	0.02230 ± 0.00021^a	0.94	3.045
Planck + 3 ν	0.02236 ± 0.00015	0.67	3.045
(D + CMB)	0.02224 ± 0.00022	0.99	2.95 ± 0.22
(D + Y_p)	0.0221 ± 0.0006	2.71	$2.86^{+0.28}_{-0.27}$

Implications:

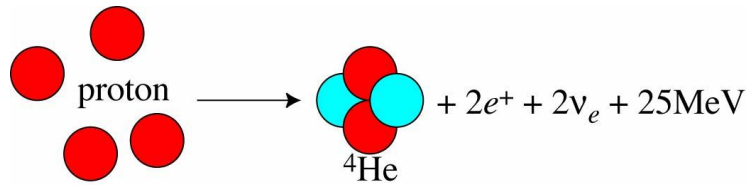
Baryonic matter represents only a few percent of the critical density

There are only 3 active neutrino species

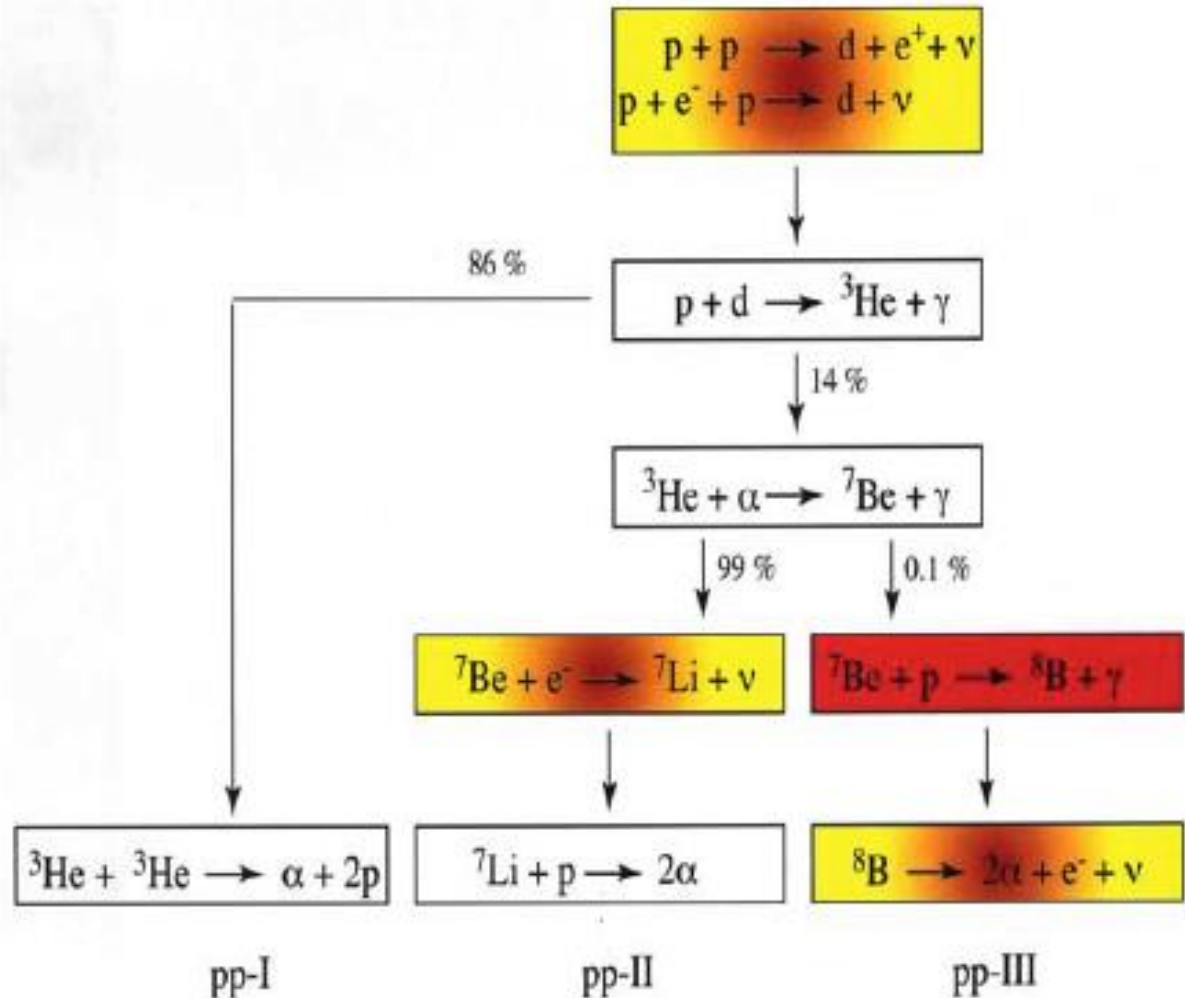
Hertzprung-Russell Diagram



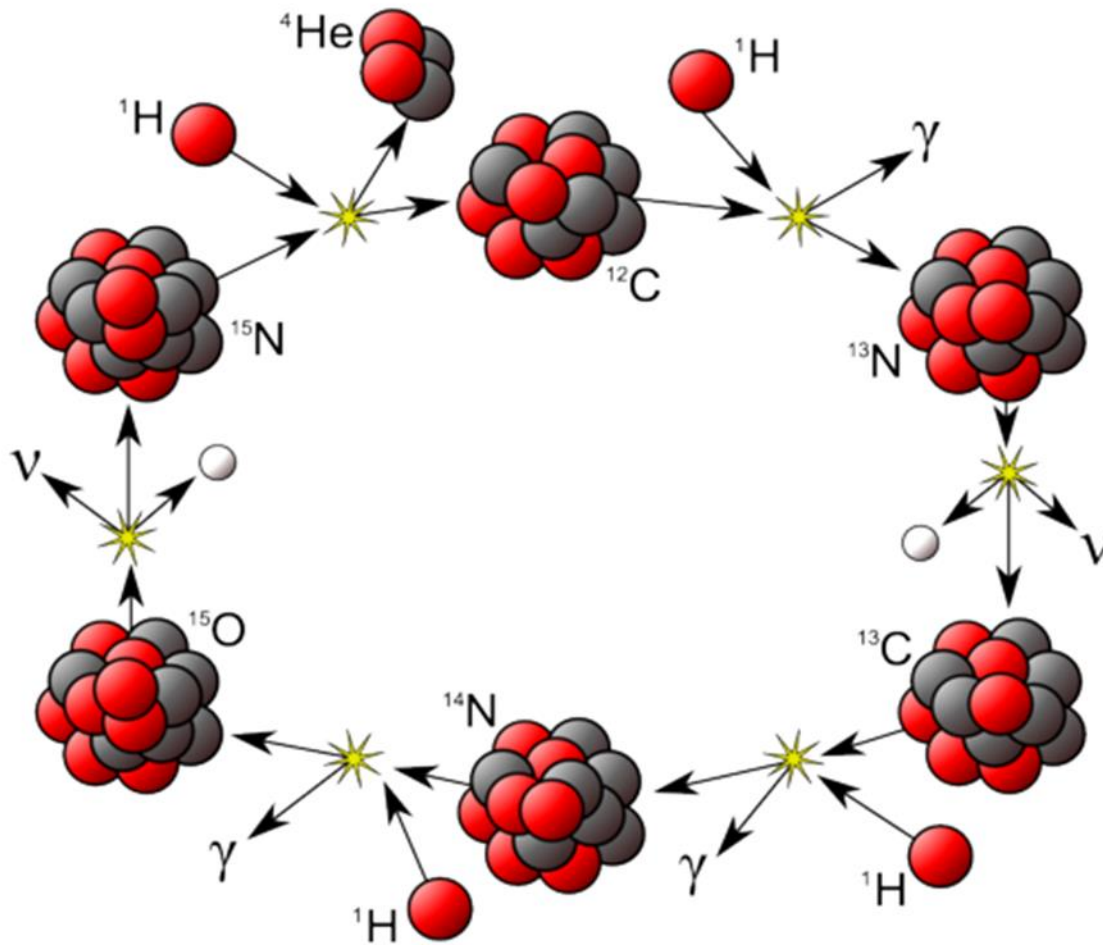
The Sun shines by nuclear fusion reactions!



Hans Bethe
Nobel Prize 1967



CNO Cycle

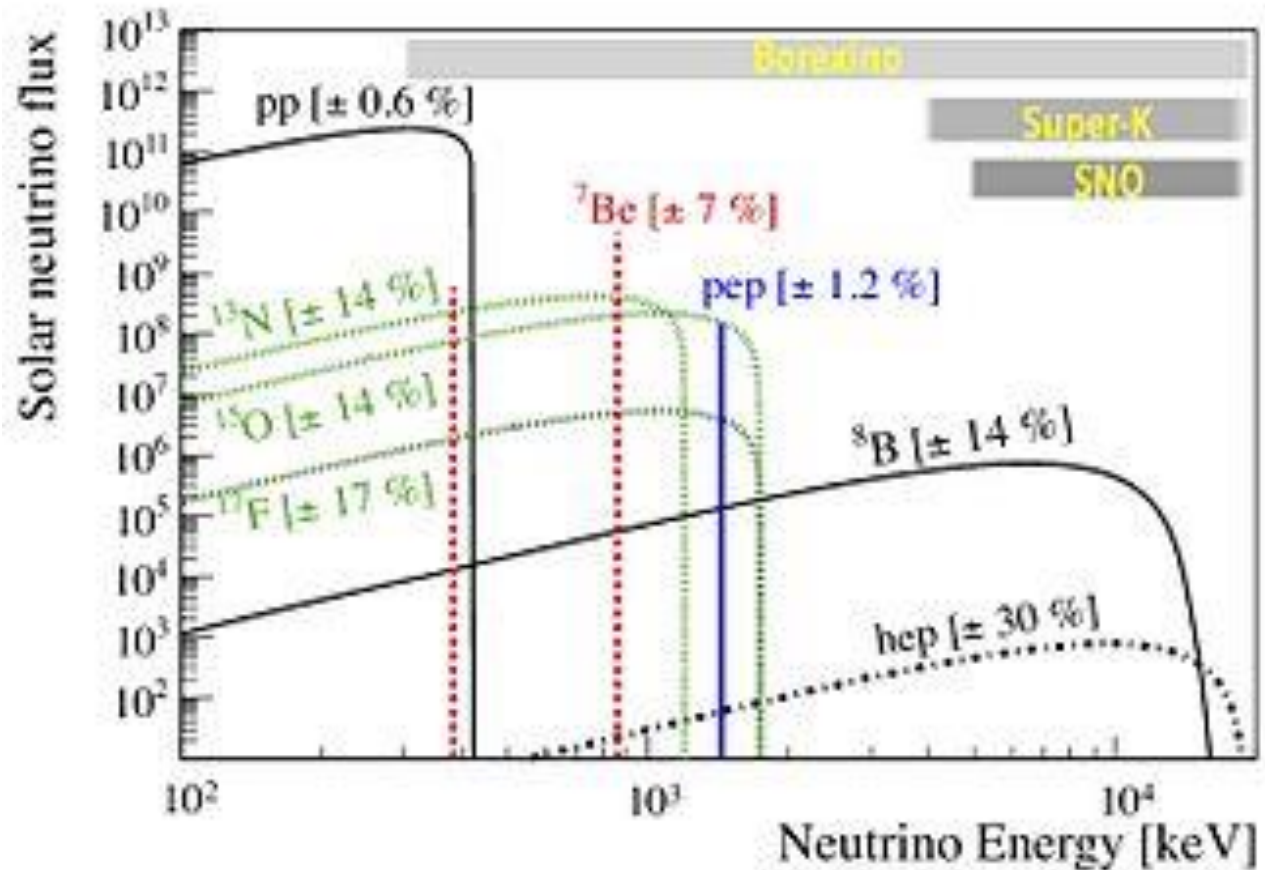


Main hydrogen
burning
mechanism in
more massive
stars

Predicted fluxes of solar neutrinos at Earth



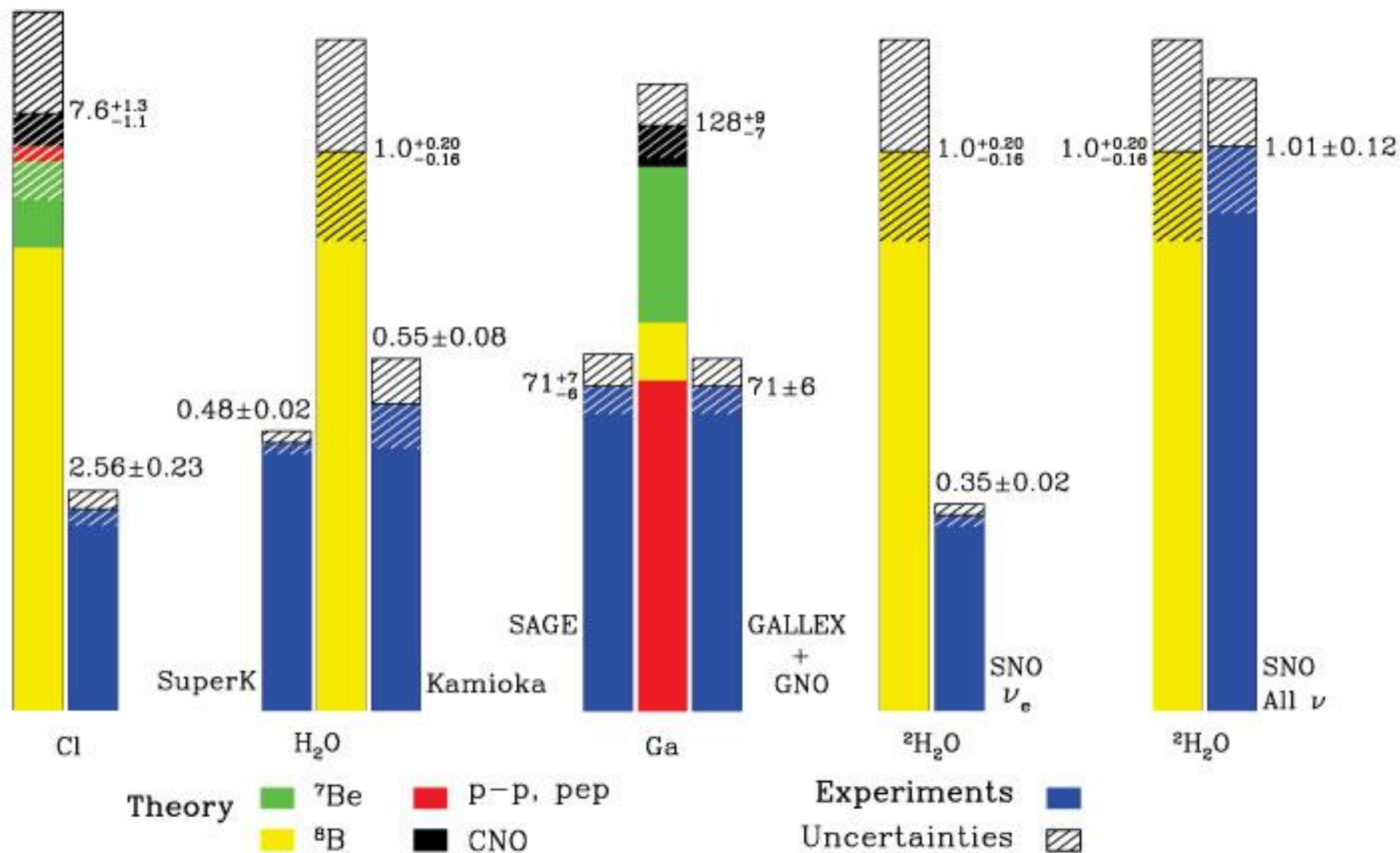
John Bahcall



$$\Phi_{\nu} = 2 \times L_{\text{sun}}/Q \quad \text{and} \quad L_{\text{sun}} = 1.2 \text{ kW/m}^2$$
$$Q = 25 \text{ MeV} \quad \rightarrow \quad \Phi_{\nu} = 6 \times 10^{10} / \text{cm}^2 / \text{sec}$$

Total Rates: Standard Model vs. Experiment

Bahcall-Pinsonneault 2000



Recent Observations of Solar pp, pep, ${}^7\text{Be}$, and CNO Neutrinos by Borexino Collaboration

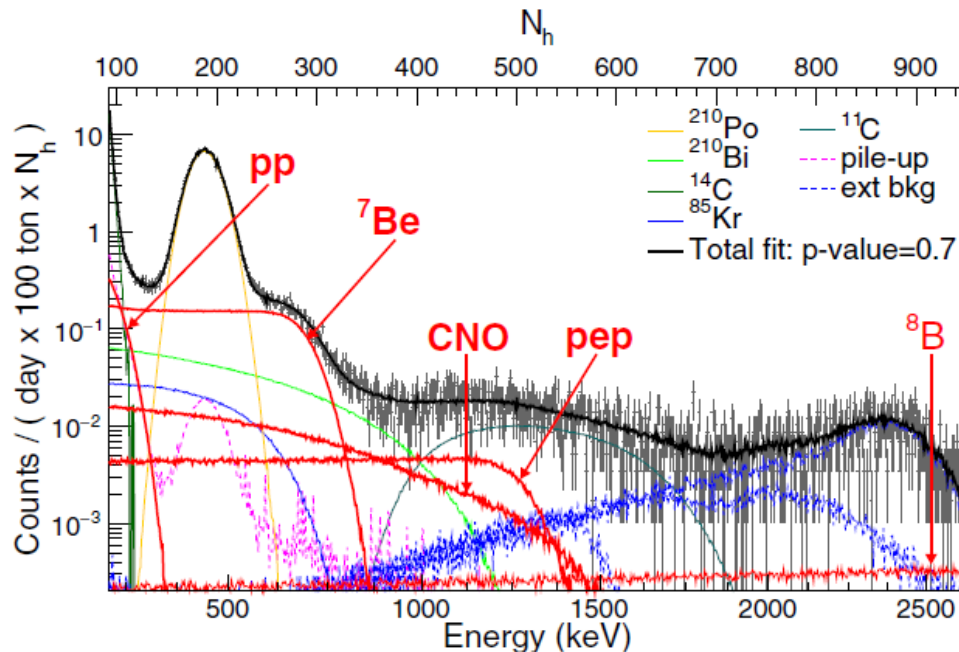
$$\Phi_{\nu pp} = (6.1 \pm 0.5^{+0.3}_{-0.5}) \times 10^{10} \text{ cm}^{-2} \text{ s}^{-1}$$

$$\Phi_{\nu pep} = (1.27 \pm 0.19^{+0.08}_{-0.12}) \times 10^8 \text{ cm}^{-2} \text{ s}^{-1}$$

$$\Phi_{\nu {}^7\text{Be}} = (4.99 \pm 0.11^{+0.06}_{-0.08}) \times 10^9 \text{ cm}^{-2} \text{ s}^{-1}$$

Nature **512** (2014) 383

Phys. Rev. D **100** (2019) 082004



$$\Phi_{\nu \text{CNO}} = 7.0^{+3.0}_{-2.0} \times 10^8 \text{ cm}^{-2} \text{ s}^{-1}$$

Nature **587** (2020) 577

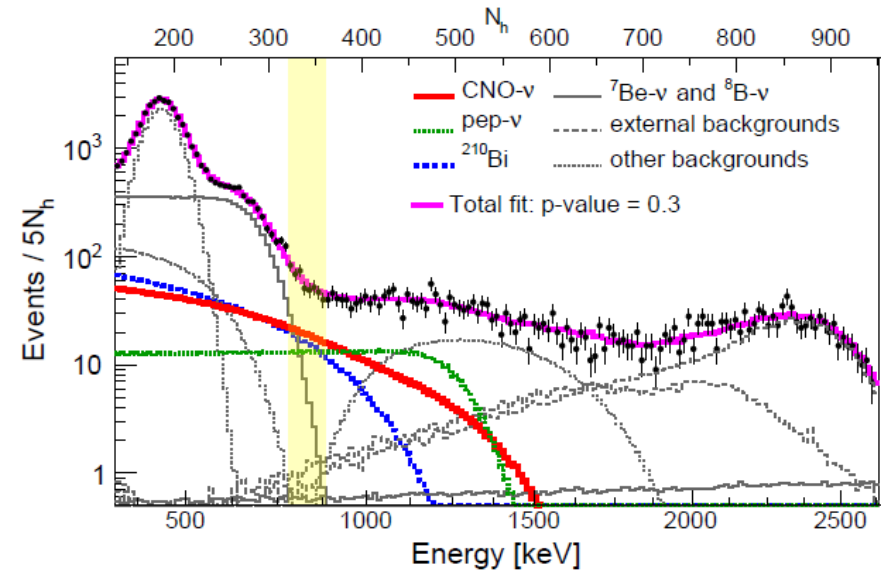
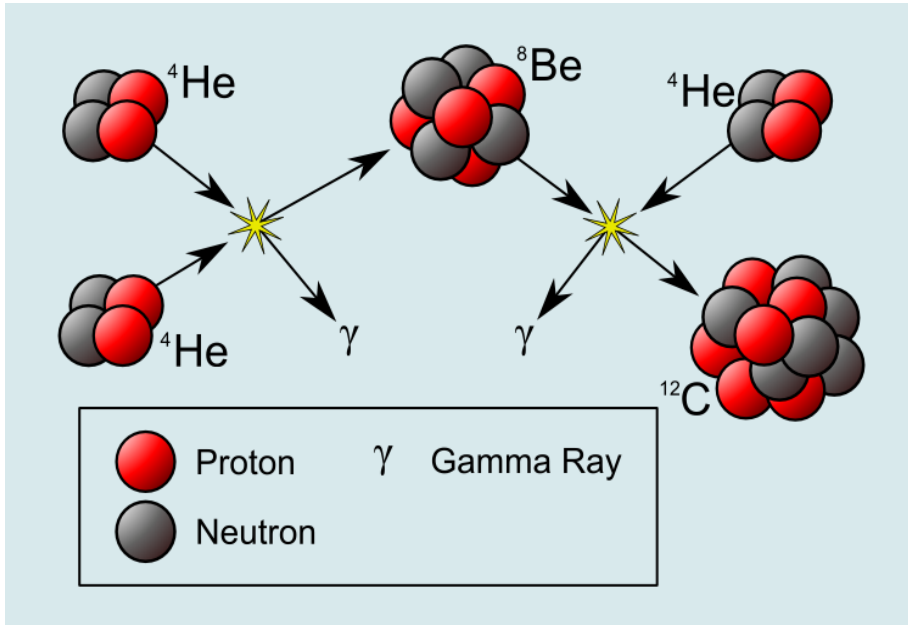


Figure 2: Energy distribution of Borexino events (black points) and spectral fit (magenta). CNO- ν , ${}^{210}\text{Bi}$, and pep- ν are highlighted in solid red, dashed blue, and dotted green, respectively. All other components are in grey. The yellow band represents the region with the largest signal-to-background ratio for CNO- ν .

Helium Burning in Red-Giant Stars



$$t_{1/2}({}^8\text{Be}) = 10^{-16} \text{ sec}$$

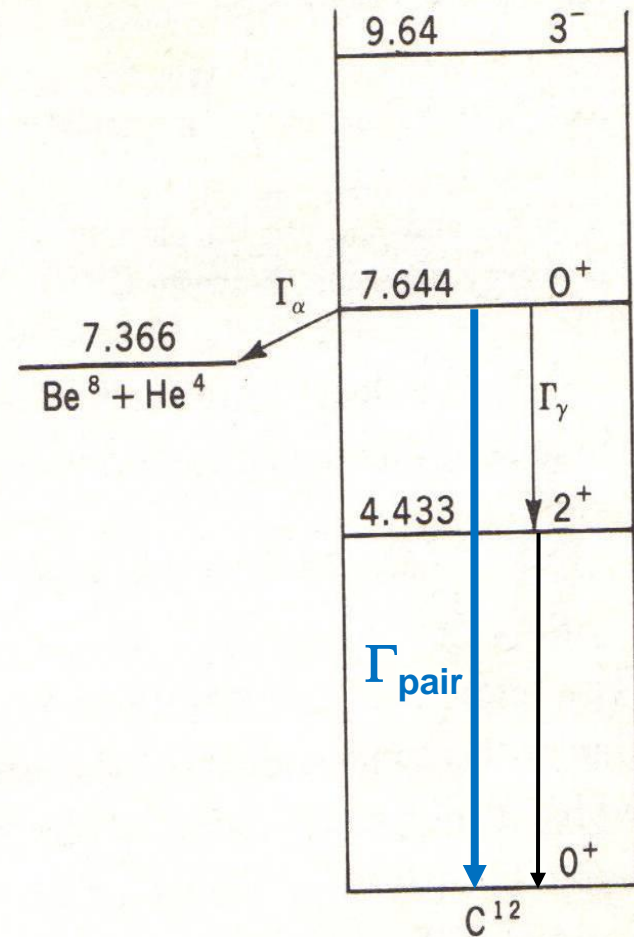
At $T = 1 \times 10^8 \text{ K}$ and $\rho = 10^5 \text{ g/cc}$:
 $N({}^8\text{Be})/N({}^4\text{He}) = 1 \times 10^{-9}$



Burbidge, Burbidge, Fowler, Hoyle
B²FH (1957)

Fig. 5-18 The energy-level diagram of C^{12} . Alpha particles may fuse with the transient Be^8 nuclei to form the 7.644-Mev state of C^{12} . This state usually breaks up by rejecting the alpha particle, but with a smaller probability it also decays electromagnetically to the 4.433-Mev state.

Clayton



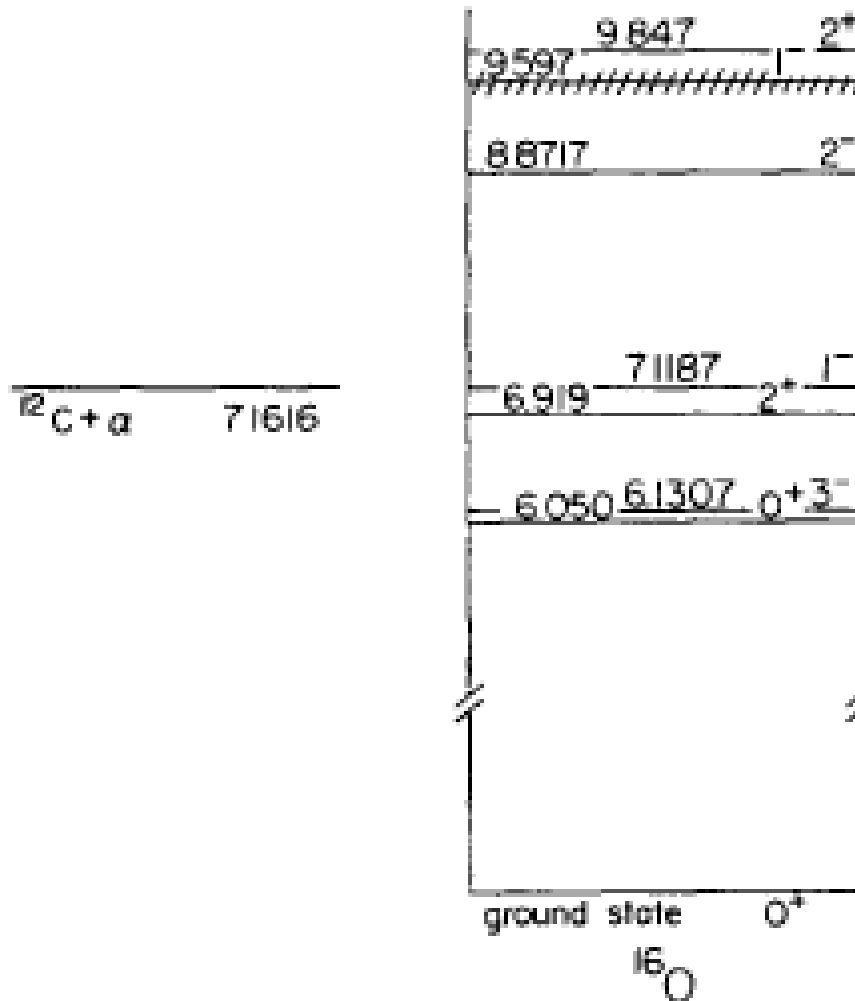
**See talk by Tibor Kibedi and
Phys. Rev. Lett. 182 (2020) 182701
for recent measurements of Γ_{pair} , Γ_γ**

THE $^{12}\text{C}(\alpha, \gamma)^{16}\text{O}$ REACTION AND STELLAR HELIUM BURNING †

P. DYER and C. A. BARNES

California Institute of Technology, Pasadena, California 91109

Nuclear Physics A
233 (1974) 495



Subthreshold
 1^- state plays
major role in
 ^{16}O production

Fig. 1. Lowest states of the ^{16}O nucleus ^{3).}

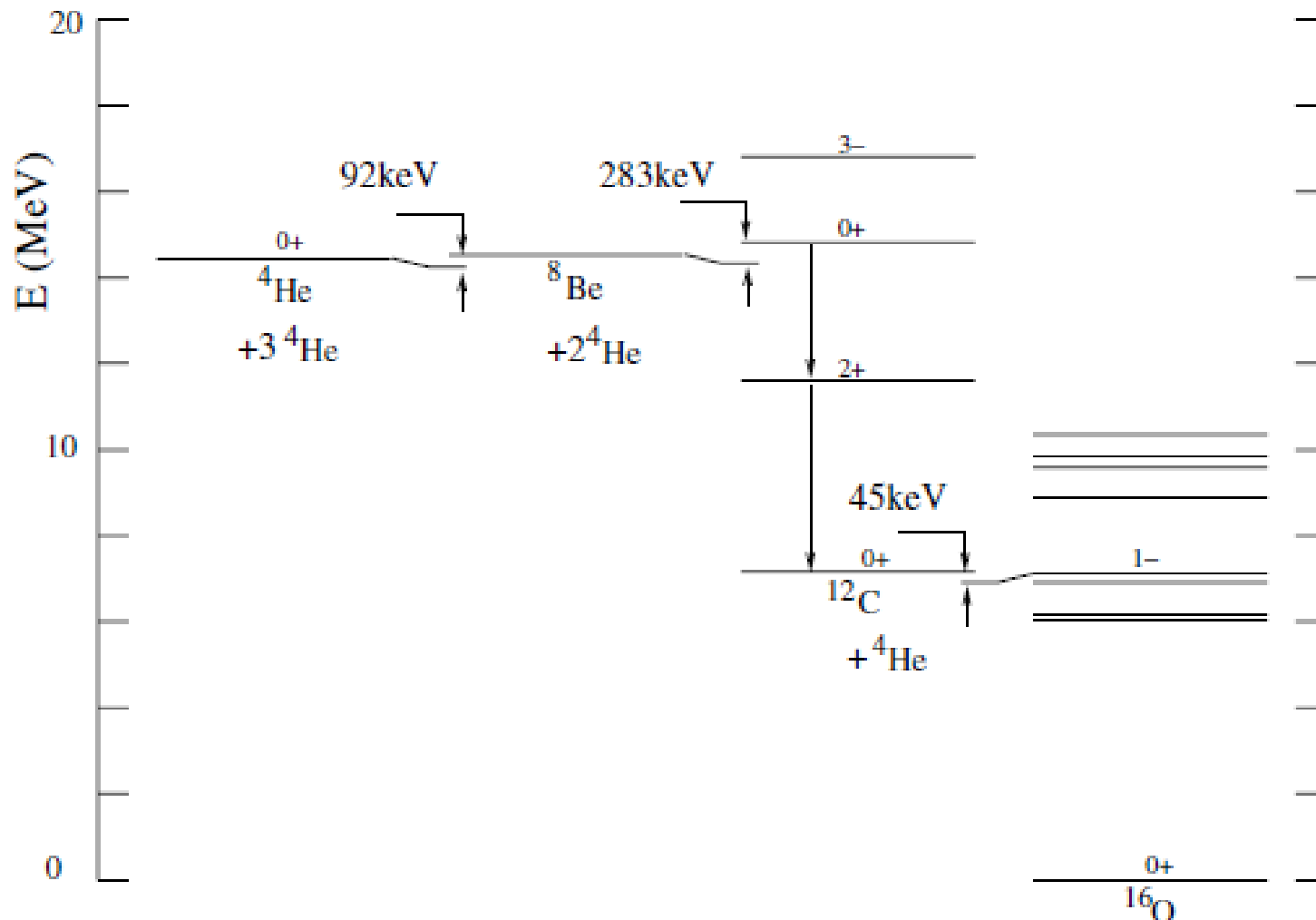


Fig. 8.5. The energy levels of four ^4He nuclei.

Basdevant *et al.* argue that this arrangement of nuclear levels is the only one that allows for significant amounts of ^{12}C to be produced in stars. (Fundamentals in Nuclear Physics, Springer, 2005)

Fate of Stars

For stars with masses $< 10 M_{\text{Sun}}$

No further nuclear reactions possible

→ White Dwarf (maximum mass = $1.4 M_{\text{Sun}}$)

Chandrasekhar Mass limit

Supported by electron degeneracy pressure

For more massive stars,

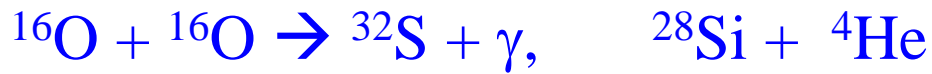
No such quiet fate possible

→ Neutron Star or Black Hole



Subrahmanyan
Chandrasekhar
Nobel Prize 1983

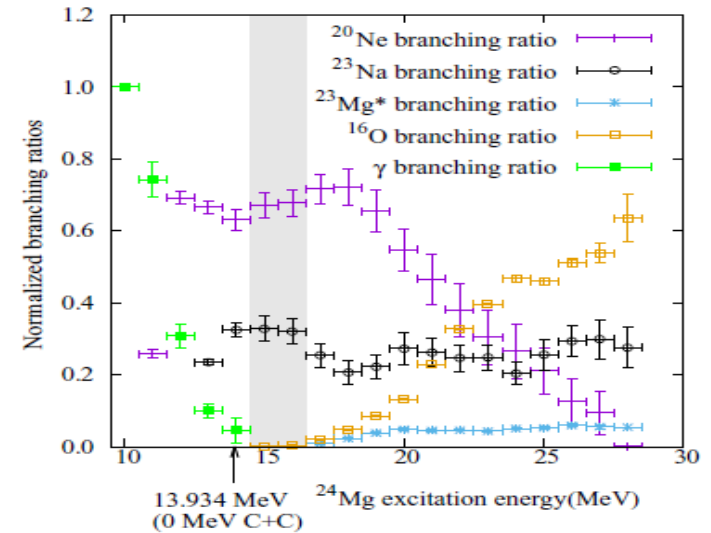
Advanced stellar burning



PHYSICAL REVIEW C 95, 015805 (2017)

Decay branching ratios of excited ^{24}Mg

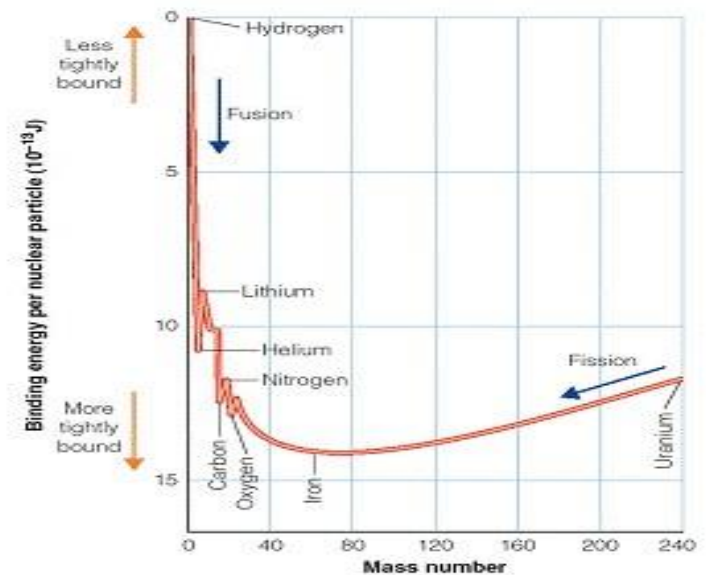
J. M. Munson *et al.*



Then through successive captures of ^4He ,

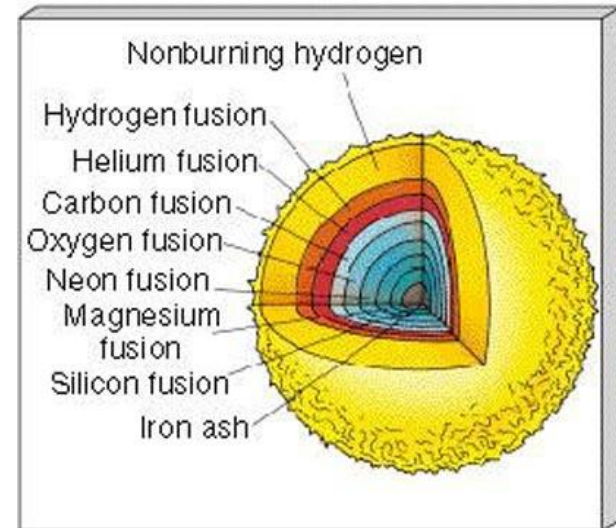


At this point the star is on its deathbed,
No further energy generation possible



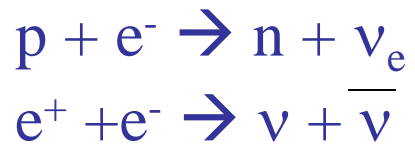
Late stage massive star

Burning Stage	Temperature (keV)	Density (g/cm ³)	Timescale
Hydrogen	5	5	7×10^6 years
Helium	20	700	5×10^5 years
Carbon	80	2×10^5	600 years
Neon	150	4×10^6	1 year
Oxygen	200	1×10^7	6 months
Silicon	350	3×10^7	1 day
Collapse	600	3×10^9	seconds
Bounce	3000	10^{14}	milliseconds
Explosion	100 - 600	varies	0.1 – 10 seconds



Supernova Explosion

Temperature goes up
Density goes up

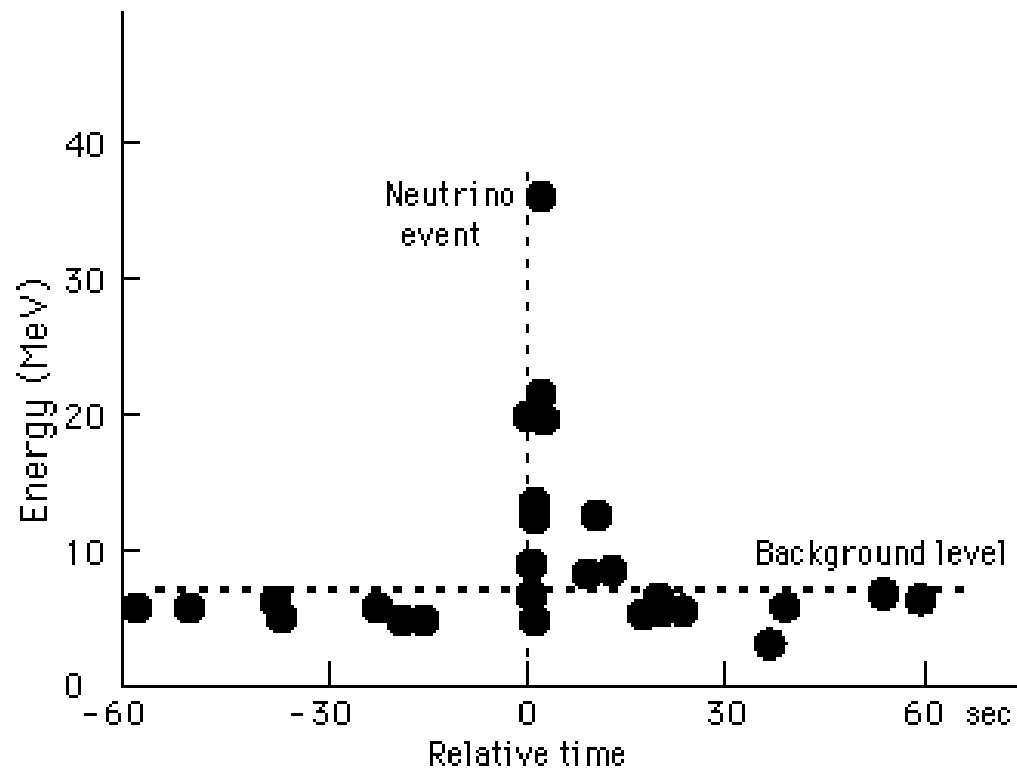
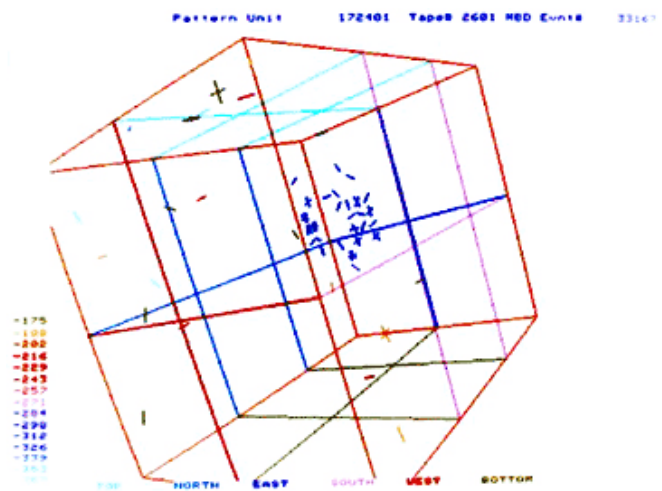


99% of SN energy
comes off in neutrinos

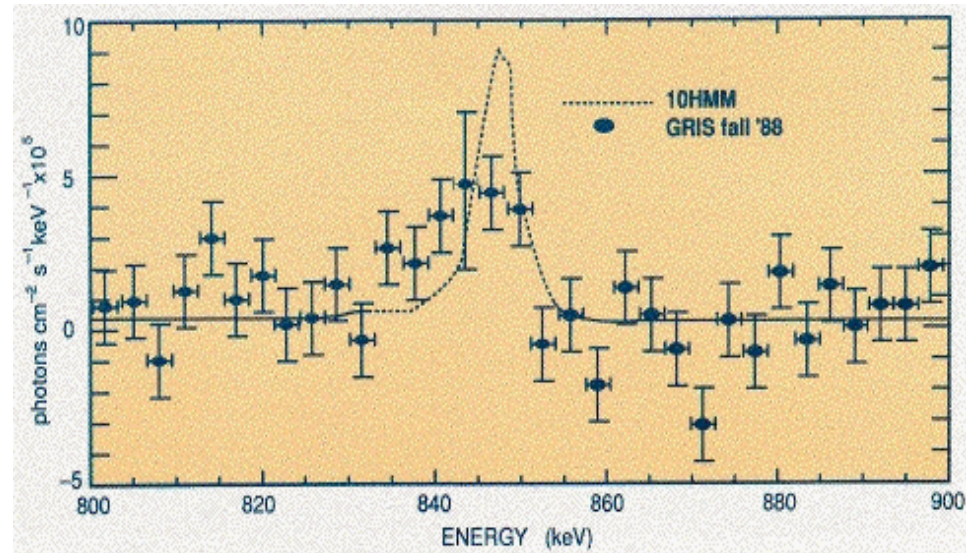
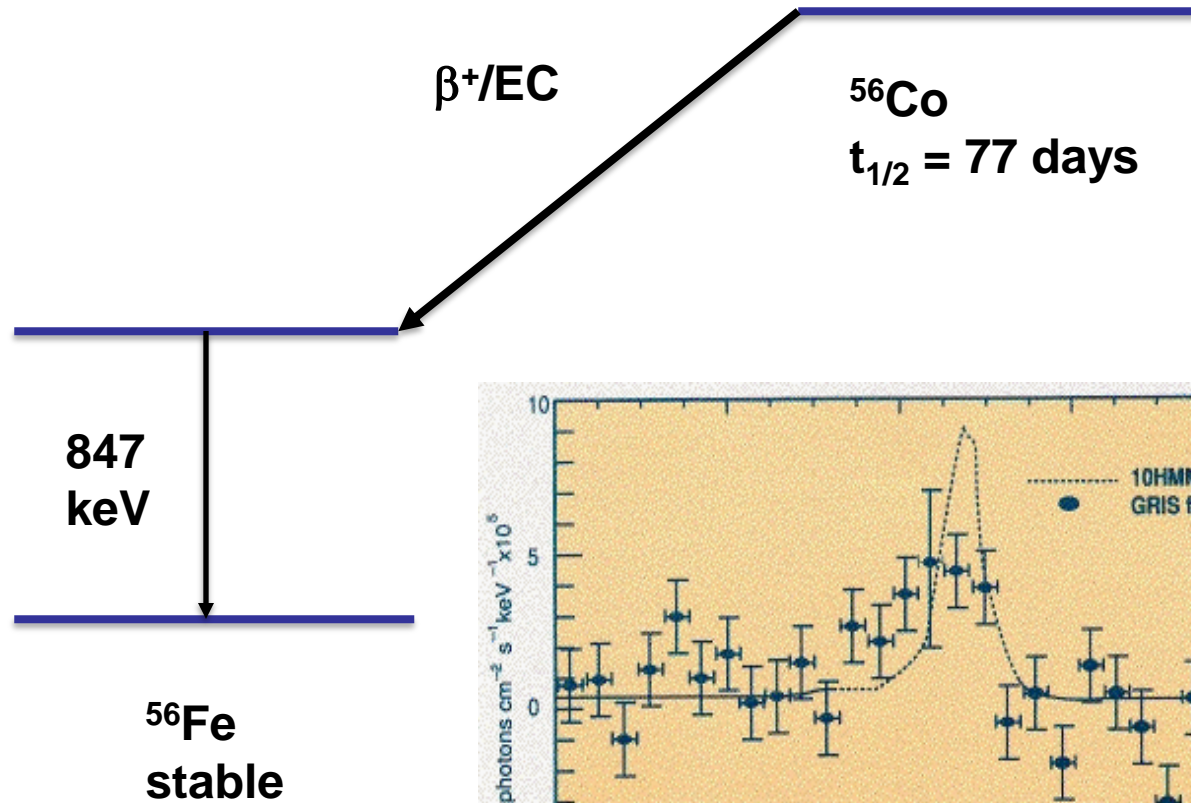


SN 1987a

Neutrinos from SN1987a observed by Kamiokande and IMB underground telescopes



^{56}Co gamma rays observed from SN1987a

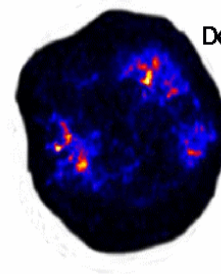
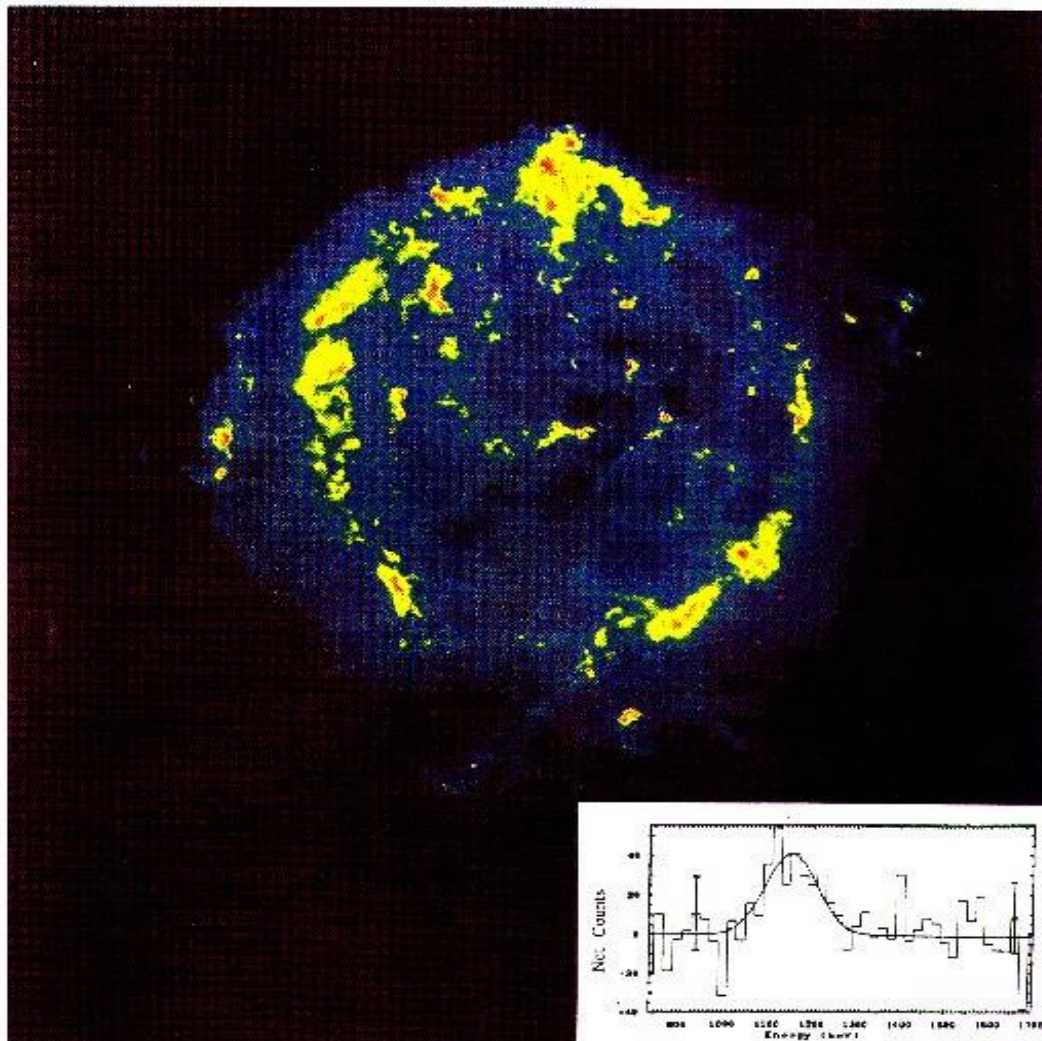


$t_{1/2}(^{56}\text{Co}) = 77.08 \pm 0.08$ days

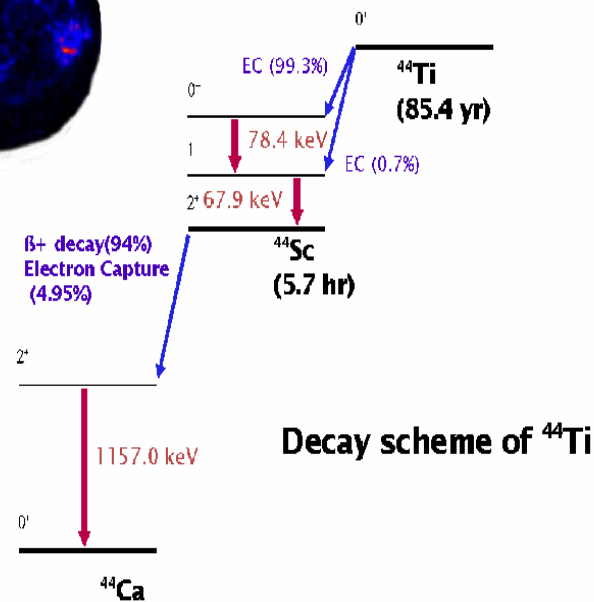
Lesko *et al.*

PRC **40** (1989) 445

^{44}Ti gamma rays observed from CasA

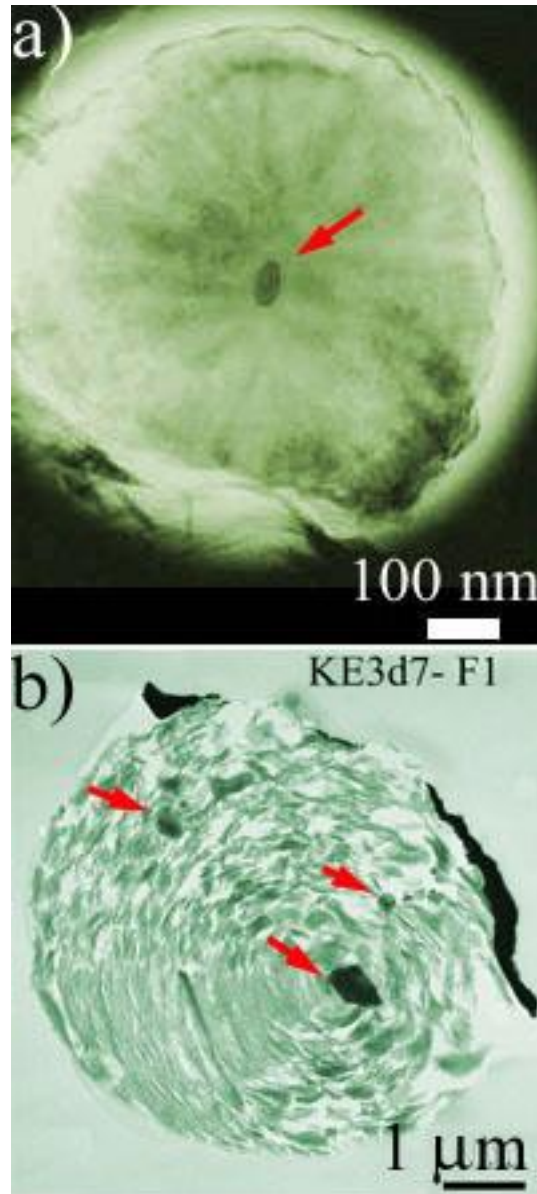


Detection of the nuclear decay lines of ^{44}Ti in Cas A
Jacco Vink (Columbia University)



$t_{1/2}(^{44}\text{Ti}) = 62 \pm 2$ years
 Norman *et al.*
 PRC **57**(1998) 2010

$\sigma(^{40}\text{Ca}(\alpha, \gamma)^{44}\text{Ti})$
 R.D. Hoffman *et al.*
 Ap. J. **715**(2010) 1383



**Pre-solar
graphite grains
from Murchison
meteorite
containing TiC
inclusions**

E. Zinner *et al.*
Washington Univ.

Isotopic properties of silicon carbide X grains from the Murchison meteorite in the size range 0.5–1.5 μm

PETER HOPPE^{1,2*}, ROGER STREBEL^{1,2}, PETER EBERHARDT², SACHIKO AMARI^{3,4} AND ROY S. LEWIS⁴

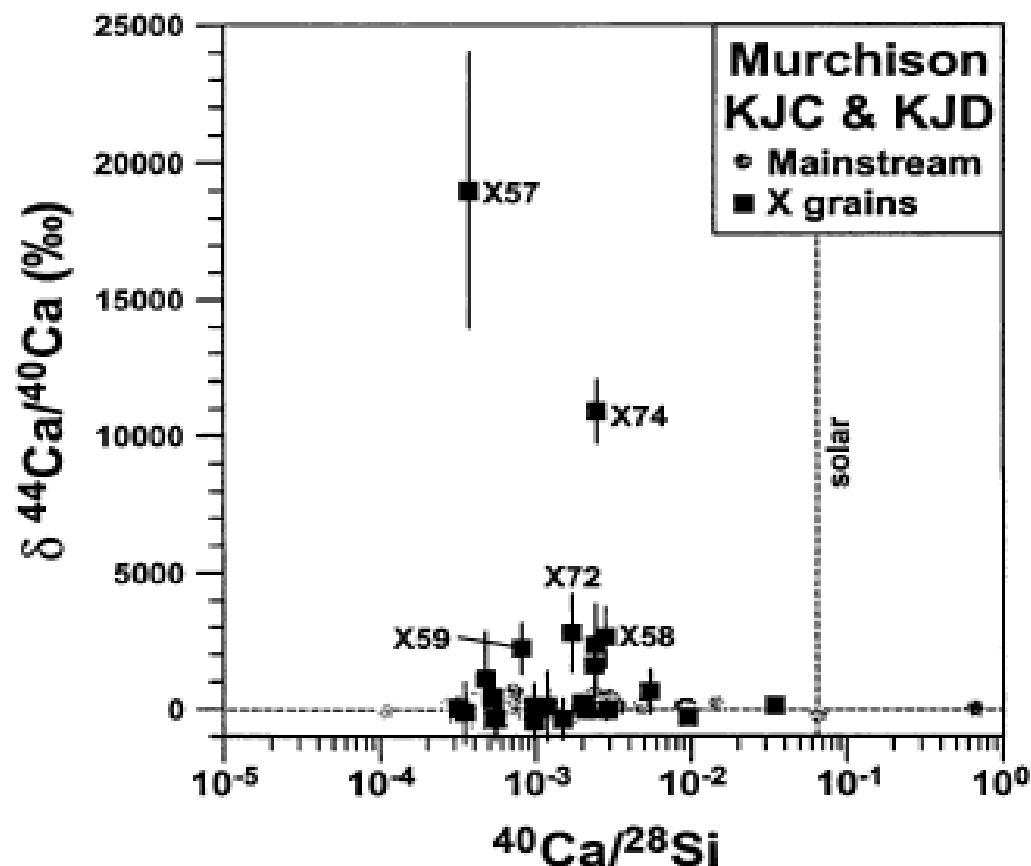


FIG. 8. Calcium-44 and Ca/Si ratios in presolar SiC grains from the Murchison separates KJC and KJD. $\delta^{44}\text{Ca}/^{40}\text{Ca} = [(^{44}\text{Ca}/^{40}\text{Ca})/(^{44}\text{Ca}/^{40}\text{Ca})_{\odot} - 1] \times 1000$ with $(^{44}\text{Ca}/^{40}\text{Ca})_{\odot} = 0.0212$. Errors are 1σ . Five X grains (X57, X58, X59, X72, X74) have large excesses in ^{44}Ca by factors between 3 and 20, indicative of extinct ^{44}Ti . A few other X grains are enriched in ^{44}Ca by up to a factor of 3, but errors are large for those grains.

Supernova Remnants

- Neutron star – supported by neutron degeneracy pressure
 - Upper limit on neutron star mass $\sim 2.5 M_{\text{Sun}}$
Oppenheimer-Volkoff limit

Higher masses \rightarrow black hole

$$R_{\text{Schwarzschild}} = 2GM/c^2$$

$$\text{For } 1 M_{\text{Sun}}, \quad R_s = 3 \text{ km}$$

Origin of Heavy elements

Neutron capture reactions

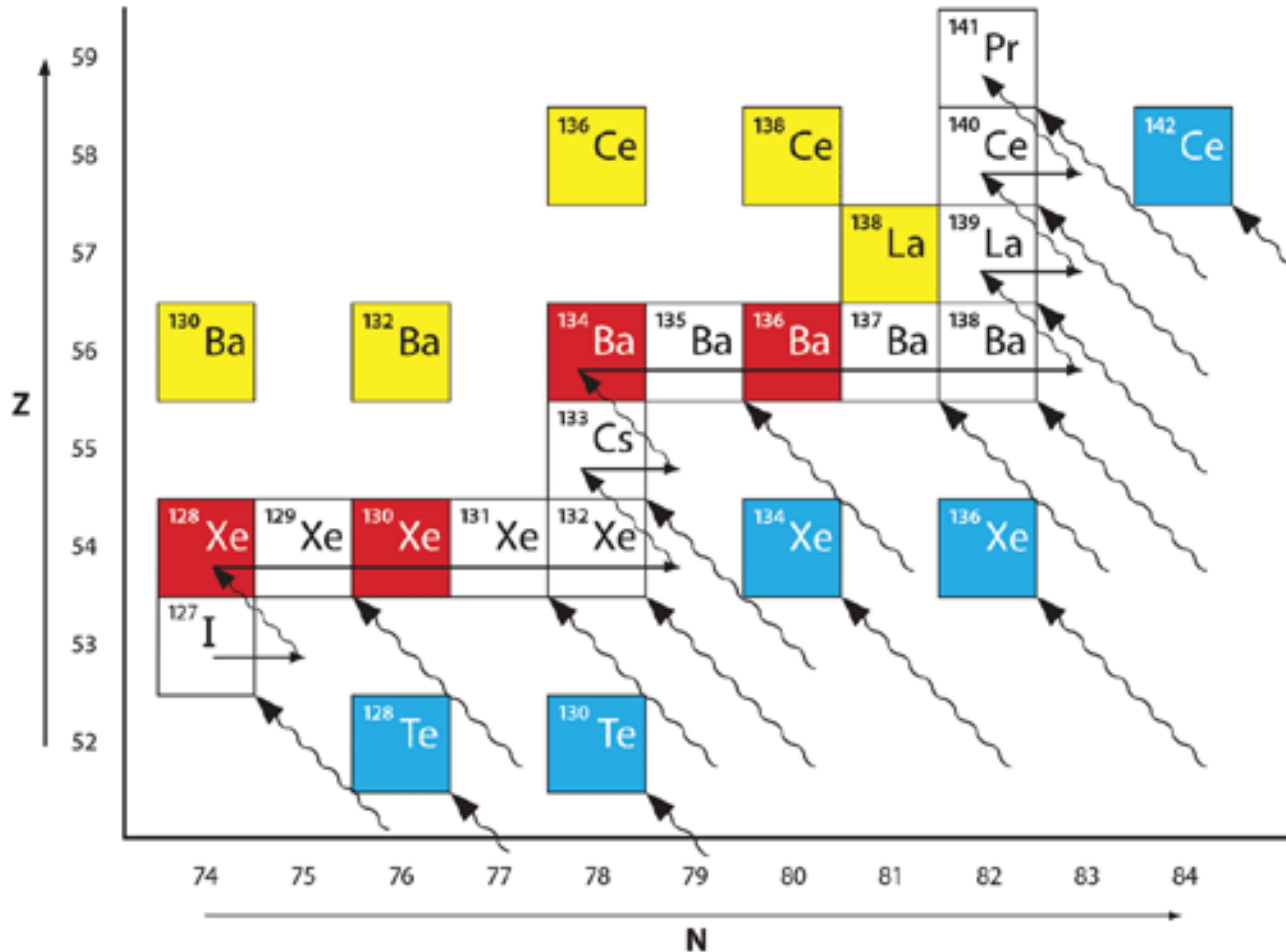
slow (s) process

produces half of nuclei from $^{56}\text{Fe} \rightarrow ^{209}\text{Bi}$
occurs during He-burning in red giant stars

rapid (r) process

produces other half of nuclei heavier than
 ^{56}Fe plus Th and U
occurs in supernovae, neutron star mergers ?

s and r processes



Blue – r process only
Red – s process only
White – s and r processes
Yellow – p process

s – process

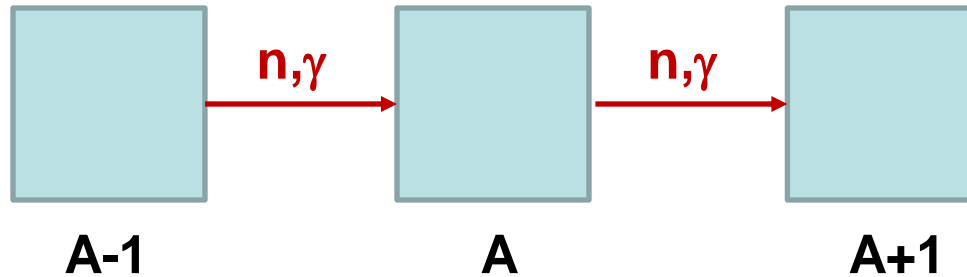
Believed to occur during He-burning in red giant stars

Neutron sources : $^{13}\text{C}(\alpha,n)^{16}\text{O}$, $^{22}\text{Ne}(\alpha,n)^{25}\text{Mg}$ reactions

at $T \sim (1 - 4) \times 10^8 \text{ K}$, $n_n \sim 10^8 / \text{cm}^3$

$$\rightarrow r_{n\gamma} = n_n \langle \sigma v \rangle = (10^8 / \text{cm}^3)(10^{-25} \text{ cm}^2)(2 \times 10^8 \text{ cm/s}) = 2 \times 10^{-9} / \text{s}$$

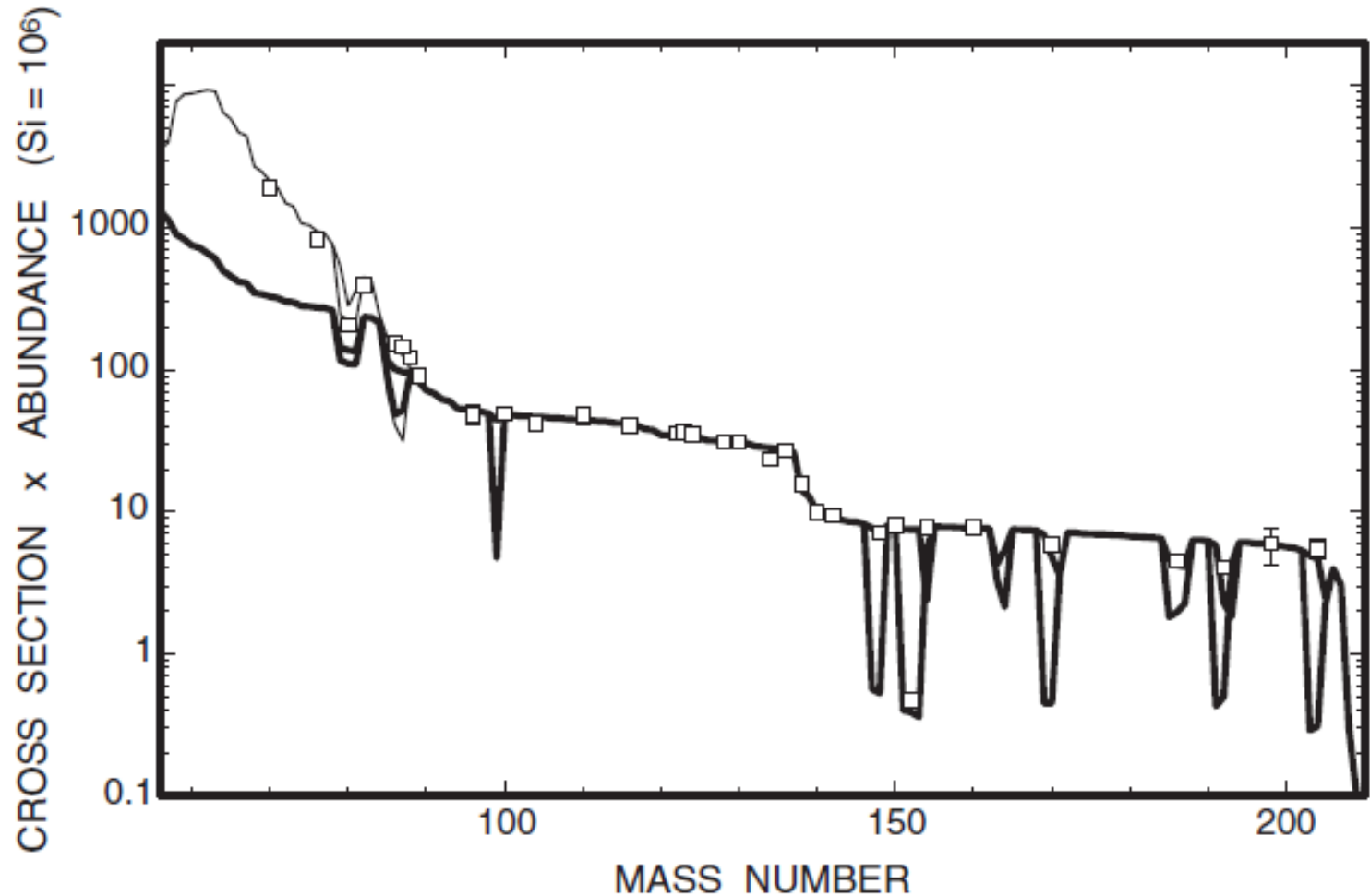
$$\rightarrow \tau_{n\gamma} \sim 15 \text{ years !}$$



$$dN_A/dt = \sigma_{A-1}N_{A-1} - \sigma_A N_A$$

At equilibrium, $dN_A/dt = 0$

→ expect $\sigma_{A-1}N_{A-1} = \sigma_A N_A = \text{constant}$



→s-process abundance peaks for nuclei with low $\sigma(n,\gamma)$

→i.e. $N = 50, 82, 126$ → $A \sim 90, 140, 208$

Termination of s-process

At207 ^{9/-} 1.81 h ϵ β^+ γ 814.4, 588.3, 300.7, ... α 5.758 E 3.91	At208 ⁶⁺ 1.63 h ϵ β^+ γ 686.5, 660.0, 177.6, ... α 5.641 ω , ... E 4.98	At209 ^{9/-} 5.4 h ϵ γ 545.0, 781.9, 790.2, ... α 5.647, ... E 3.49	At210 (5+) ⁺ 8.1 h ϵ γ 1181.4, 245.3, 1483.3, ... α 5.524 ω , 5.442, 5.361, ... γ 83 (ω), 106, ... E 3.98	At211 ^{9/-} 7.21 h ϵ γ 687.0 ω α 5.868, ... γ 669.6 ω , ... E .786 210.987481	(9-) At212 (1-) ⁻ 119 ms 312 ms α 7.837, α 7.681, ... 7.897, 7.618, ... γ 62.9 ω , e- 211.990735	At213 ^{9/-} 0.12 μ s α 9.08 212.99292	9- At214 1- ⁻ 0.76 μ s 0.56 μ s α 8.78, α 8.819, 213.99636
Po206 8.8 d ϵ γ 1032.3, 511.3, 286.4, 807.4, ... α 5.223 E 1.85	19/- Po207 5/- ⁻ 2.8 s 5.80 h IT 268.1 γ 814.5D, 300.5D ϵ β^+ .89 (ω), 1.14, 992.3, 742.6, 911.8, ... α 5.115 ω E 2.91	Po208 2.898 a α 5.115, ... ϵ ω γ 291.8 $\nu\omega$, 570.1, 601.5, ... 207.981231	Po209 1/+ ⁻ 102 a α 4.880, ... γ 260.5 ω , 262.8 ϵ γ 896.1 ω 208.982416	Po210 RaF 138.38 d α 5.3044 ... γ 803.1 $\nu\omega$ σ_γ (.5 mb+ .0.03) $\sigma_\alpha < 2$ mb 209.982857	(25+) Po211 9/+ ⁺ 25.2 s AcC' 0.516 s α 7.27, 8.88, ... α 7.451, ... γ 569.2D, 569.2D ω , 1063.1D, 897.2, ... IT ω 210.986637	(18+) Po212 45 s ThC' 0.298 μ s α 11.65, ... γ 2614.4, 583.0 IT -36 211.988852	Po213 9/+ ⁺ 3.8 μ s α 8.376, ... γ 778.8 ω 212.992843
Bi205 9/- ⁻ 15.31 d ϵ β^+ .98 ω γ 1764.3, 703.5, 987.6D, ... E 2.71	Bi206 ⁶⁺ 6.243 d ϵ β^+ .98 $\nu\omega$ γ 803.1, 881.0, 516.2, ... E 3.76	Bi207 9/- ⁻ 32 a ϵ β^+ ω γ 569.7, 1063.7D, ... E 2.398	Bi208 (5+) ⁺ 3.68E5 ϵ γ 2614.4 E 2.879	Bi209 9/- ⁻ 100 σ_γ (10 mb+24 mb), 0.19 $\sigma_\alpha < .3$ μ b 208.980383	9- Bi210 1- ⁻ RaE 5.01 d α 4.946, 4.908, β^- 1.162, 1.648 $\nu\omega$, 4.687 γ 266.2, 309.2, ... γ 305 $\nu\omega$, 266 σ_α .05, 0.2 E 1.162	Bi211 9/- ⁻ AcC 2.14 m α 6.623, 6.279 γ 351.1 β^- ω 210.98726	(15-) Bi212 1(-) ⁻ 7 m ThC β^- - 1.009 h β^- 2.251, ... γ 727.3 α 6.34, α 6.051, ... γ 39.9, ... E 2.254 σ_α 211.991272
9- Pb204 1.12 h 1.4 IT 911.7, ... γ 899.2, 374.8, ... σ_γ 0.70, 2.0 203.973029	Pb205 5/- ⁻ 1.5E7 a ϵ no γ σ_γ 4.5 E 0.051	Pb206 24.1 RaG σ_γ .027, 205.974449	13/+ Pb207 1/- ⁻ 0.80 s 22.1 IT 1063.7 γ 569.7 AcD σ_γ .70, .38 206.975881	Pb208 ThD 57.4 σ_γ 0.49 mb, 2.0 mb σ_α 8. ... 207.976636	Pb209 9/+ ⁺ 3.25 h β^- .645 no γ E .644	Pb210 RaD 22.3 a β^- .017, .061 γ 46.5, e- α 3.72 $\nu\omega$ σ_γ 0.5 E .0635	Pb211 9/+ ⁺ AcB 36.1 m β^- 1.38, ... γ 404.9, 831.9, 427.0, ... E 1.37
Tl203 1/+ ⁺ 29.524 σ_γ 11.4, 41 $\sigma_\alpha < .3$ mb 202.972329	Tl204 2- ⁻ 3.78 a β^- .7634 no γ ϵ σ_γ 22, 9E1 E -.7637 E+.347	Tl205 1/+ ⁺ 70.476 σ_γ 0.10, 0.7 204.974412	(12-) Tl206 0- ⁻ 3.74 m RaF IT 1025.564 γ 687, 453, 217, 266.2, ... β^- 1.528, ... γ 803.1 ω E 1.534	11/- Tl207 1/+ ⁺ 1.3 s AcC'' 4.77 m IT 997.1, ... γ 351.0 β^- 1.44, ... γ 897.2 ω , ... E 1.42	Tl208 5(+) ⁺ ThC'' 3.053 m β^- 1.796, 1.28, 1.52, ... γ 2614.5, 583.2, 510.7, ... E 5.001	Tl209 (1+) ⁺ 2.16 m β^- 1.8, ... γ 1567.0, 465.1, 117.2, ... E 3.98	Tl210 (5+) ⁺ RaC'' 1.30 m β^- 1.9, 1.3, 2.3, ... γ 799.7, 298, ... (n) E 5.49

122

124

126

128

r-process needed to explain Th , U

r-process path

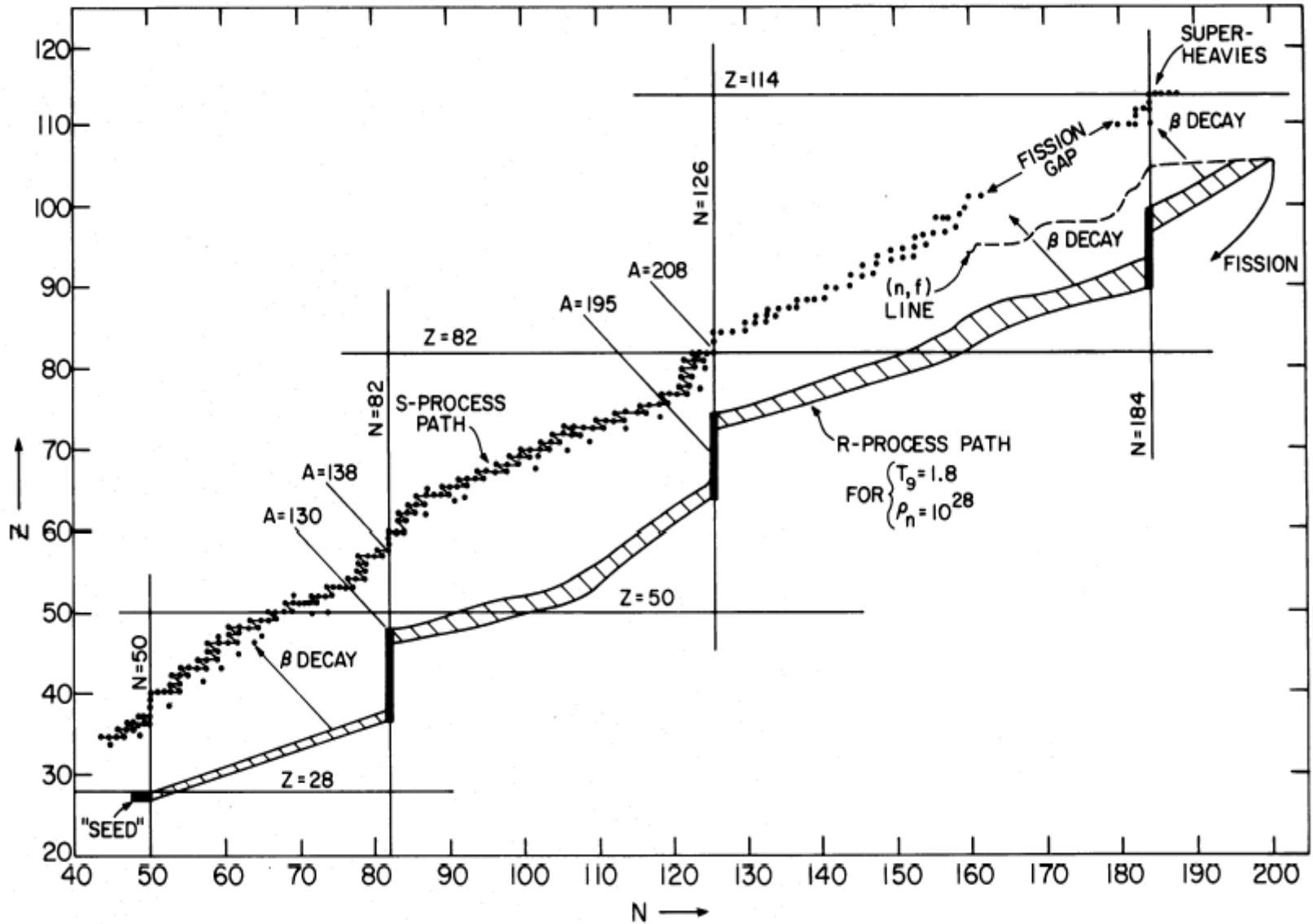
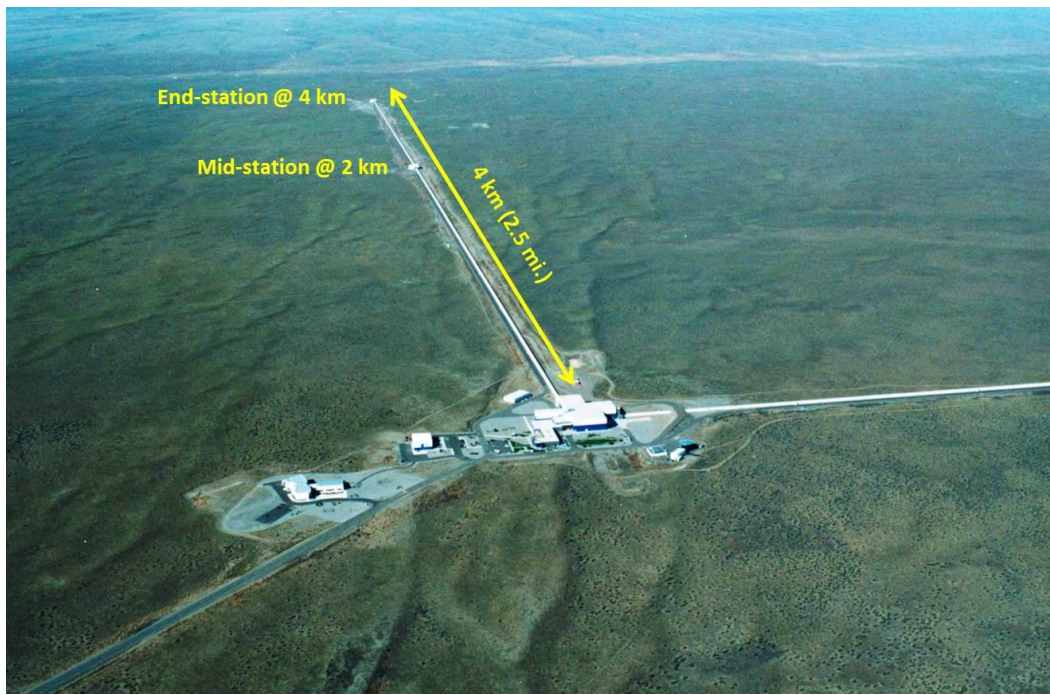


FIG. 1.—Neutron capture paths for the *s*-process and the *r*-process. The *r*-process was computed for initial conditions of $T_9 = 1.8$ and $n_n = 10^{28}$ (Schramm and Norman 1976).



GW170817: Observation of
Gravitational Waves from a Binary
Neutron Star Inspiral
LIGO, PRL **119** (2017) 161101

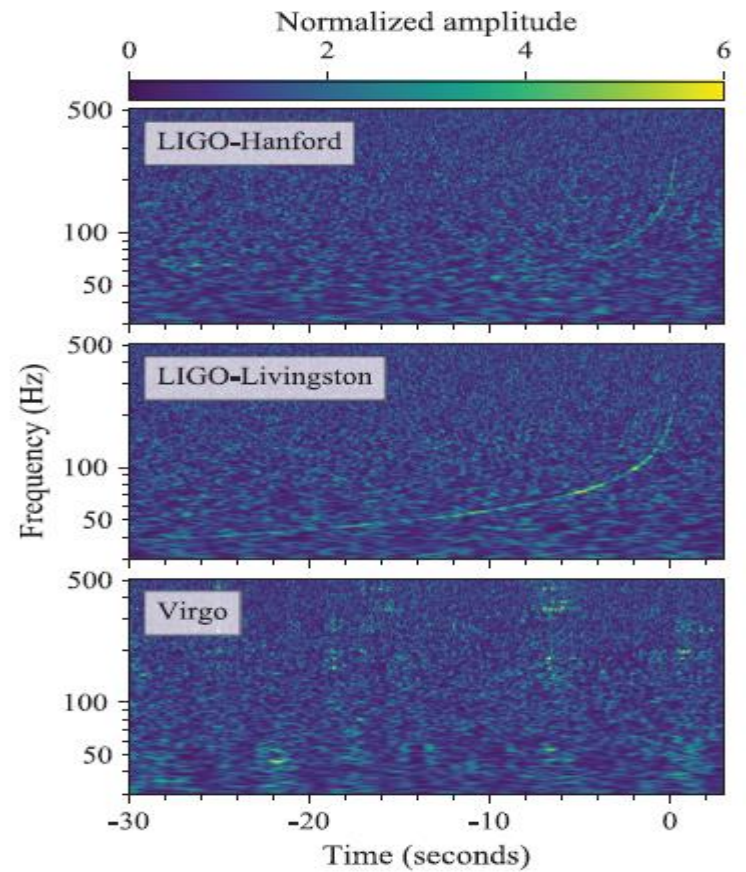
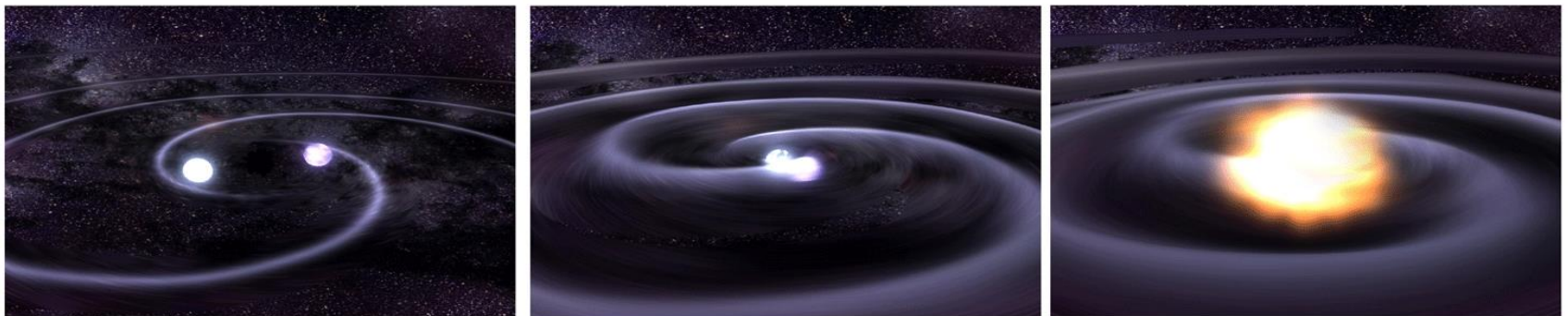
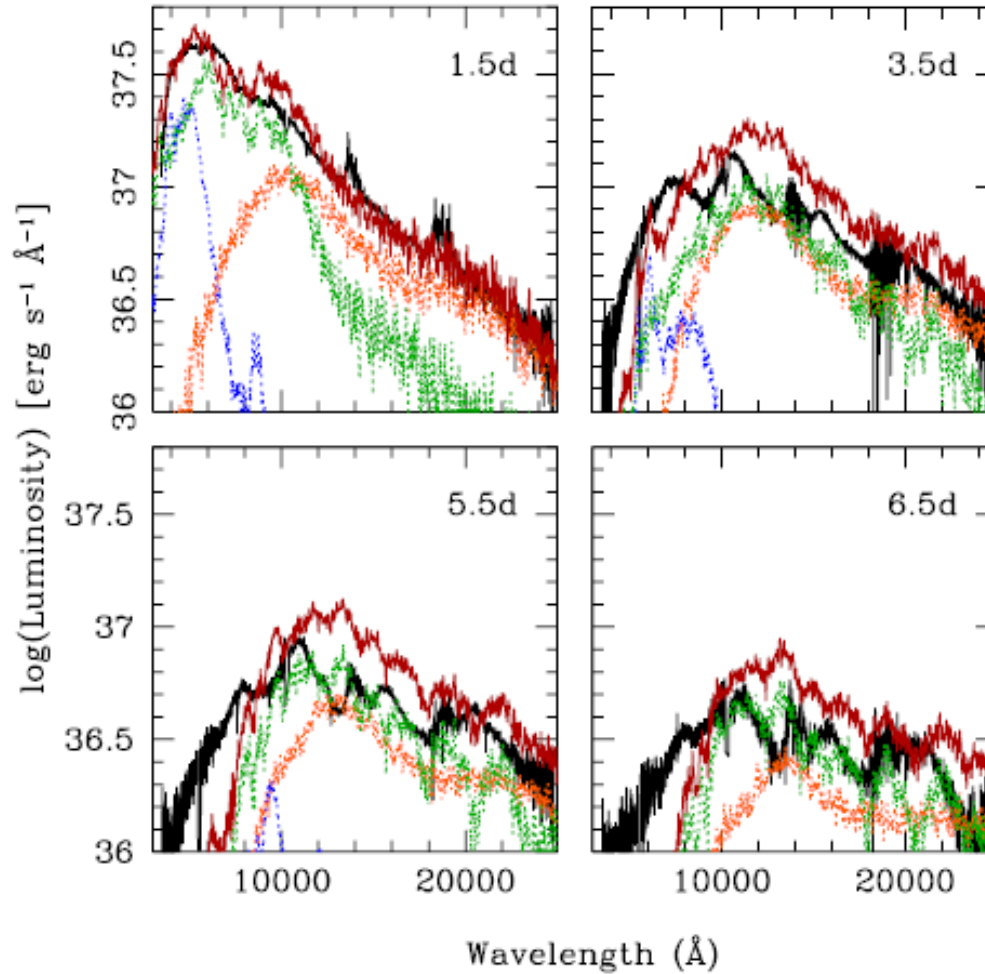


FIG. 1. Time-frequency representations [65] of data containing the gravitational-wave event GW170817, observed by the LIGO-Hanford (top), LIGO-Livingston (middle), and Virgo (bottom) detectors. Times are shown relative to August 17, 2017 12:41:04



Evidence for neutron-star mergers as a possible site for the r-process



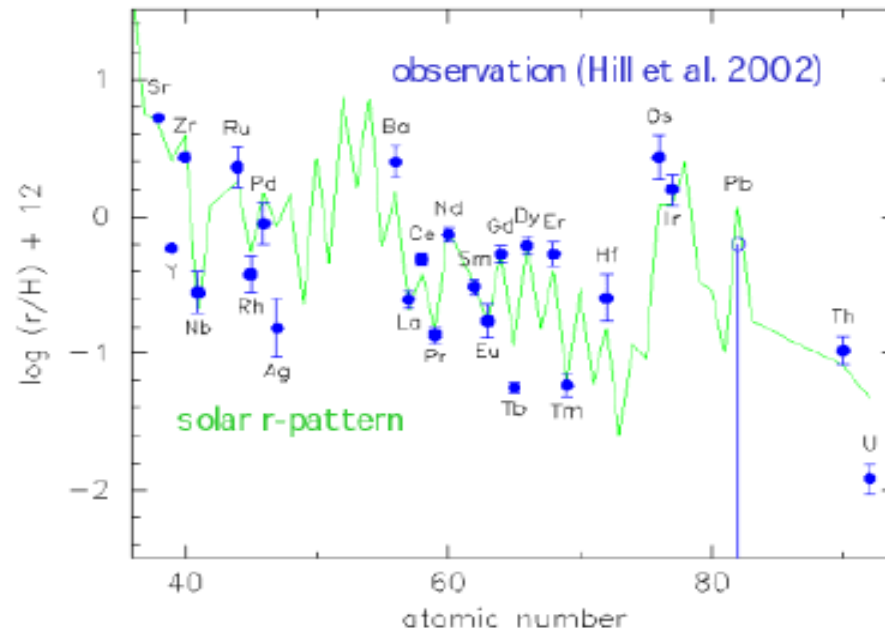
Orange curves are rich in lanthanides (indicative of r-process)

Photon spectra observed from GW170817 and GRB170817 sources

Discovery of U in an extremely metal-poor star !

CS 31082-001, $[Fe/H] = -2.9$ (Cayrel et al. 2001)

- ➡ good news: new cosmochronometer U-Th (with, e.g., Th-Eu)
- ➡ bad news: "non-universality" up to Th and U



Wanajo et al

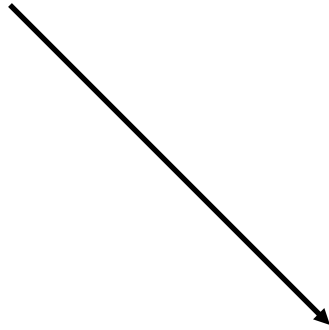
U-Th cosmochronology

age of CS 31082-001 hard lower limit on the age of the universe

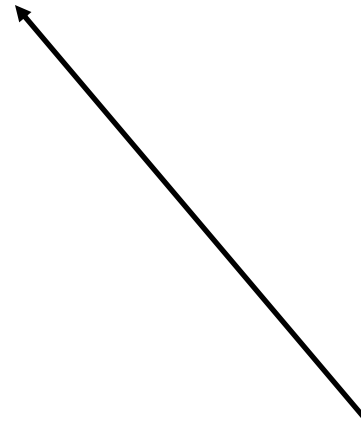
$$t^*(U/Th) = 14.1 \text{ G yr}$$

This star may have formed too early for neutron-star mergers to explain r-process abundances. Thus, there may be more than one r-process site.

Source of stellar energies



Nuclear reactions



Origin of chemical elements